Title

Integral Experiment on Polyethylene Using Radiative Capture and Inelastic Excitation in Indium Foils inside a D-D High Flux Neutron Generator.

Author

Nnamani, Nnaemeka

Publication Date

2019

Peer reviewed|Thesis/dissertation

Integral Experiment on Polyethylene Using Radiative Capture and Inelastic Excitation in Indium Foils inside a D-D High Flux Neutron Generator.

By

Nnaemeka Nnamani

A dissertation submitted in partial satisfaction of the

requirements for the degree of

Doctor of Philosophy

in

Nuclear Engineering

in the

Graduate Division

of the

University of California, Berkeley

Committee in charge:

Professor Karl Van Bibber, Co-Chair
Professor Lee A. Bernstein, Co-Chair
Professor Paul R. Renne

Spring 2019

Integral Experiment on Polyethylene Using Radiative Capture and Inelastic Excitation in Indium Foils inside a D-D High Flux Neutron Generator.

by

Nnaemeka Nnamani

Abstract

Integral Experiment on Polyethylene Using Radiative Capture and Inelastic Excitation in Indium Foils inside a D-D High Flux Neutron Generator.

By

Nnaemeka Nnamani

Doctor of Philosophy in Nuclear Engineering

University of California, Berkeley

Professor Karl Van Bibber, Co-Chair

Professor Lee A. Bernstein, Co-Chair

Cross-sections nuclear data are invaluable to the nuclear community. As well as providing information on nuclear structure of matter and reaction dynamics, they provide practical support for applications including design and modelling of fission and fusion reactors, shielding geometry for radiation sources such as radiation treatment machines, etc. Evaluated cross section data in form of evaluated nuclear data are the products of experiment and theoretical modelling. Before they can be used, their reliability and accuracy need to be assured. This is done through integral experiments in which prediction from simulation using the evaluated nuclear data is compared to experimental value.

Integral benchmark experiments are used to test the accuracy and reliability of evaluated nuclear data. They are a rich source of information with which a wide range of validation and comparison exercises can be made [1]. Such benchmark experiments provide global measures of data performance for applications and are a valuable resource for nuclear data testing and evaluation efforts [2]. Integral experiments in reactors play an essential role in nuclear data validation and improvements [3].

Applications of integral benchmark experiments are found in fission and fusion reactors designs for safety, in fast neutron therapy for shielding calculation. They are a very powerful means of assessing the quality of nuclear data for specific applications, nicely complementing differential measurements [4].

Neutron generators such as D-D fusion generators can serve the purpose of performing integral benchmark experiment for validation of cross-section data. The

Nuclear Engineering department of the University of California Berkeley has D-D neutron generator called the High Flux Neutron Generator (HFNG). It operates in the range of 100-125 keV of accelerating voltage. The generator produces neutron current of the order of 10^8 per second. These neutrons have energies between 2.2 – 2.8 MeV.

In this work, neutron elastic and inelastic scattering cross sections on carbon and hydrogen nuclear data in the evaluated nuclear database ENDF/B-VII.1 are compared to experiments via the observation of radiative capture and inelastic excitation of two long-lived isomeric state in ^{116}In and ^{115}In on a foil mounted in the center of the HFNG in order to benchmark scattering on a polyethylene moderator surrounding the generator.

Two different methods were used: single and double ratios of the products of the two reactions. Results from both methods show generally good agreement with the expected values, although some statistically significant differences are observed. These results highlight the utility of compact DD neutron sources such as the HFNG as integral benchmarks and suggest that further work should be done to improve the evaluation of scattering data on polyethylene due to its important role in shielding applications.

To:

My father, for dedication to my education

and

Goodluck Ebele Azikiwe Jonathan GCFR GCON for his value for education.

Table of Contents

List of Figures

List of Tables

Acknowledgments

I would like to thank God for the gift of life and mercy which made this work possible, as well as Professor Karl Van Bibber for his mentorship. Karl, this work will not have been possible if not for your patience, encouragement, and direction. In the same vein, I want to thank Professor Lee Bernstein for patience, and insight into nuclear data experiment and validation. I will cherish those fruitful discussions we had in your LBNL office. Thank you Professors Paul Renne and Jasmina Vujic for serving in my thesis and candidacy committees respectively.

I would also like to thank my wife for bearing with the many time I had to come home from school late and for being a pillar of support throughout the whole journey. Acknowledgement is also due to my former colleagues Leo Kirsh and Cory Waltz for being a fantastic pair to work with. Thanks also to Mauricio Unzueta and Joe Bauer for their invaluable helps in this work, and to Jonathan Morrel for his assistance during the experiments.

Lastly, I would like to thank the Federal Government of Nigeria for the scholarship that made it possible to embark on this study in the first place. Many thanks to Professor Julius Okojie of National Universities Commission for always making sure the scholarship was administered smoothly. Thanks also to Petroleum Technology Development Fund (PTDF) for taking over the administration of the scholarship.

1 Introduction

1.1 D+D Fusion reaction as a neutron source

Deuteron and tritium based neutron generators are becoming ubiquitous in research labs, particularly university research labs, due to the following reasons, among others: (1) They are relatively of low cost and easy to acquire or build. (2) They are easy to operate than the conventional research reactor making it easy to operate. (3) They produce far less radiation and radioactive waste than a conventional research reactor used as neutron source. These generators can be a good facility for the validation of nuclear data via integral experiment. With the right design, integral experiments can be easily done in the facility, thereby contributing to the validation of nuclear data used in the nuclear community. The generator in the Nuclear Engineering department of the University of California Berkley possesses this design feature.

The deuteron is the nucleus of deuterium, an isotope of hydrogen, consisting of a proton and a neutron weakly bound with a bound state energy of 2.22 MeV [5]. It has no excited state.

Two deuterons combine in nuclear fusion, in the so-called D+D reaction. This reaction was discovered when M.L.E. Oliphant, P. Harteck and Lord Rutherford were bombarding various compounds with deuterons, some of which already has deuterium in place of hydrogen [6]. They observed that protons and neutrons are emitted and went ahead to measure their energies. In addition, they observed that the probabilities of emitting protons or neutrons are equal, before the theoretical basis for why this happens was known.

The interaction of deuterons during D+D reaction proceeds via two reaction channels shown in (1.1) and (1.2).

$$ {}_{1}^{2}\mathrm{H} + {}_{1}^{2}\mathrm{H} \rightarrow {}_{2}^{3}\mathrm{He} + {}_{0}^{1}\mathrm{n} \qquad (1.1) $$

$$ {}_{1}^{2}\mathrm{H} + {}_{1}^{2}\mathrm{H} \rightarrow {}_{1}^{3}\mathrm{H} + {}_{1}^{1}\mathrm{p} \qquad (1.2) $$

D+D reaction has equal likelihood of proceeding through any of the two channels [6]. The fact that the channel probabilities are the same is due to the fact the nuclear force acting on nucleons is charge symmetric, making the probability of ejecting either neutron or proton the same [7].

1.2 The D+D fusion reaction in High Flux Neutron Generator (HFNG)

This work was done at the High Flux Neutron Generator (HFNG) in the Department of Nuclear Engineering, University of California Berkeley. The HFNG is a D-D fusion reactor in which deuterium ions produced in a multi-cusp ion source are accelerated to about 120 keV and impinges on a titanium target that is self-loading, that is the titanium target absorbs deuterons.

Neutrons produced are marked by angular dependencies of both energy and yield.

The angular distribution of emitted neutrons is given by [8] as a least square fit to experimental data in Ref [9] .

$$Y(\theta) = Y(90^o) \times \left(1 + \sum_{i=1}^{n} A_i \cos^i\theta\right) \qquad (1.3)$$

Where $Y(90^o)$ is the yield at 90^o. The parameters A_i, for i > 1 refer to the anisotropy in the yield of neutrons. This anisotropy depends on the bombarding deuteron energy. Multiplying (3) by the differential cross section at 90^0 gives the differential cross-section for reactions (1.1) and (1.2), that is:

$$\frac{d\sigma(\theta)}{d\Omega} = \sigma(90^0)Y(\theta) \qquad (1.4)$$

Using the parameters A_i for thin target at deuteron energy of 100 keV shown in Table 1.1 below, the differential cross section can be calculated and plotted as shown in Figure 1.1.

A0	A1	A2	A3	A4	A5
1	0.01741	0.88746	0.22497	0.08183	0.37225

Table 1.1. Values of A_I in (1.3)

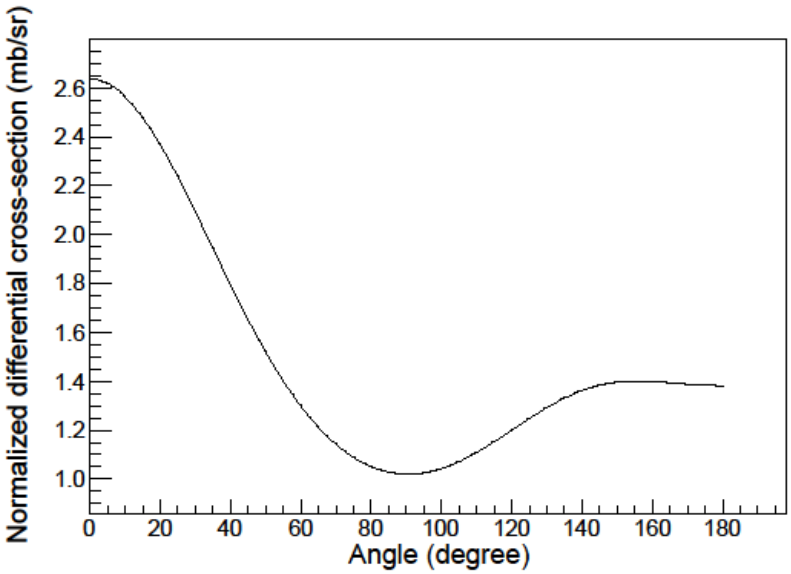

Figure 1.1. Differential cross section for D(d, n)3He at a deuteron energy of 100 keV.

As Figure 1.1 shows, neutron yield is forward peaked with the minimum yield at 90^0 to the deuteron beam.

For calculation of yield in HFNG (that is thick target yield), [8] gives the number of neutron produced per square centimeter per second in a layer thickness dx as:

$$dY(E_d) = \phi\sigma(E_d)ndx \qquad (1.5)$$

Where E_d is the deuteron energy, ϕ is the flux, n is the number of deuteron atoms per cubic centimeter in the target, $\sigma(E_d)$ is the total cross-section.
By discretizing the target and computing the energy of deuteron in the layer thickness dx using Stopping Range of Ions in Matter (SRIM) software [10], the yield in each layer can be calculated. Integrating equation 1.5 gives the total neutron yield. To get the angular distribution of yield, the total cross section, $\sigma(E_d)$ in 1.5 is replaced with the differential cross section $\sigma(E_d, \theta)$ (in barns/steradian).

$$dY(E_d, \theta) = \phi\sigma(E_d, \theta)ndx \qquad (1.6)$$

Ref [11] did the simulation with SRIM in which deuterons of energy 100 keV are incident on a titanium implanted with deuteron and the kinetic energy of the deuteron

in each layer dx is noted. The yield in the layers was integrated to get the angular distribution of yield. The differential cross-section for the reaction d(d,n) ^{3}He was calculated from 1.4.

1.3 Angular distribution probability

The D+D cross-section as a function of angle, $\sigma(\theta)$ is given by:

$$\sigma(\theta) = \int \frac{d\sigma(\theta)}{d\Omega} d\Omega \tag{1.7}$$

Where $d\Omega$ is the solid angle subtended by a detector that detects the reaction product, in this case the neutron.

$$d\Omega = \sin\theta d\theta d\phi$$

Therefore, 1.7 becomes

$$\sigma(\theta) = \int_0^{2\pi} d\phi \int_{\theta_i}^{\theta_{i+1}} \frac{d\sigma(\theta)}{d\Omega} \sin\theta d\theta = 2\pi \int_{\theta_i}^{\theta_{i+1}} \frac{d\sigma(\theta)}{d\Omega} \sin\theta d\theta$$

The above is for thin target. As such, there is need to incorporate a thick target parameter. For obvious reason, thick target yield, $dY(E_d, \theta)$, is a good choice. The yield is simply used to normalize $\sigma(\theta)$. This is what was done in [11]. Thus, probability of producing neutrons at an azimuthal angle θ is given by:

$$f(\theta) = \sigma(\theta) \frac{Y(\theta)}{\sum_{\theta=0}^{\pi} Y(\theta)} \tag{1.8}$$

1.4 Energy distribution

The energy distribution of neutrons produced in (1.1) can be calculated from kinematics consideration of conservation of total relativistic energy and linear momentum [5].

$$M_D c^2 + T_D + M_d c^2 + T_d = M_{He} c^2 + T_{He} + M_n c^2 + T_n \qquad (1.9)$$

With the reaction Q value defined as:

$$Q = T_{final} - T_{initial} \qquad (1.10)$$

$$= T_{He} + T_n - T_D - T_d \qquad (1.11)$$

Considering linear momentum along and perpendicular to the beam direction gives:

$$p_d = p_{He} \cos(\theta) + p_n \cos(\xi) \qquad (1.12)$$

$$0 = p_{He} \sin(\theta) - p_n \sin(\xi) \qquad (1.13)$$

Solution of (11), (12) and (13) gives, Ref [5],

$$T_n^{\frac{1}{2}} = \frac{(M_d M_n T_d)^{\frac{1}{2}} \cos(\theta)}{M_{He} + M_n} \pm \frac{\{M_d M_n T_d \cos^2\theta + (M_{He} M_n)[M_{He} Q + (M_Y - M_d) T_d]\}^{\frac{1}{2}}}{M_{He} + M_n} \qquad (1.14)$$

The above analysis assumes a thin target.
When a thick target is involved the stopping and scattering of deuterons can cause a definite change in the neutron energy as a function of emission angle [8]. In that case, the relationship between angular distribution of the energy of emitted neutrons can be fairly accurately approximated by fitting experimental data with Legendre polynomials. [8] gives this distribution at 100 keV as a least square fit of data from [12]

$$E_n(E_d, \theta) = E_0 + \sum_{i=1}^{n} E_i Cos^i \theta \qquad (1.15)$$

Where E_0 and E_i are constants. [8] gave the parameters E_0 and E_i for deuteron energy of 100keV. They are listed in Table 1.2 while a plot of (1.15) is shown in Figure 1.2.

E0	2.46674
E1	0.30083
E2	0.01368

Table 1.2. The constants E_0 and E_i

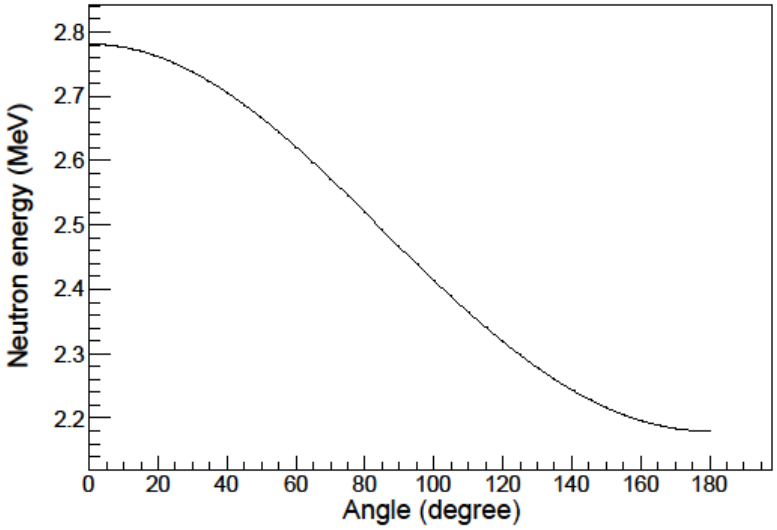

Figure 1.2. Neutron energy distribution from (1.15)

Thus, the maximum and minimum energy of neutrons produced in HFNG is approximately 2.78 MeV and 2.18 MeV respectively and occurs at 0 degrees and 180 degrees to the deuteron beam respectively.

Equations (1.8) and (1.15) were used to produce the input file for MCNP. Specifically, (1.8) was used to produce a normalized probability distribution for

angular yield of neutrons, while (1.15) was used to get the angular distribution of neutron energy. The angle runs from 0^o to 180^o in increments of 1^o.

1.5 HFNG Geometry

The Geometry of HFNG is described in [11]. Essentially, the geometry consists of two ion sources, two radio frequency sources with their matching networks, an aluminum chamber containing the target and water-cooling channels, a turbomolecular pump to keep the chamber at high vacuum.

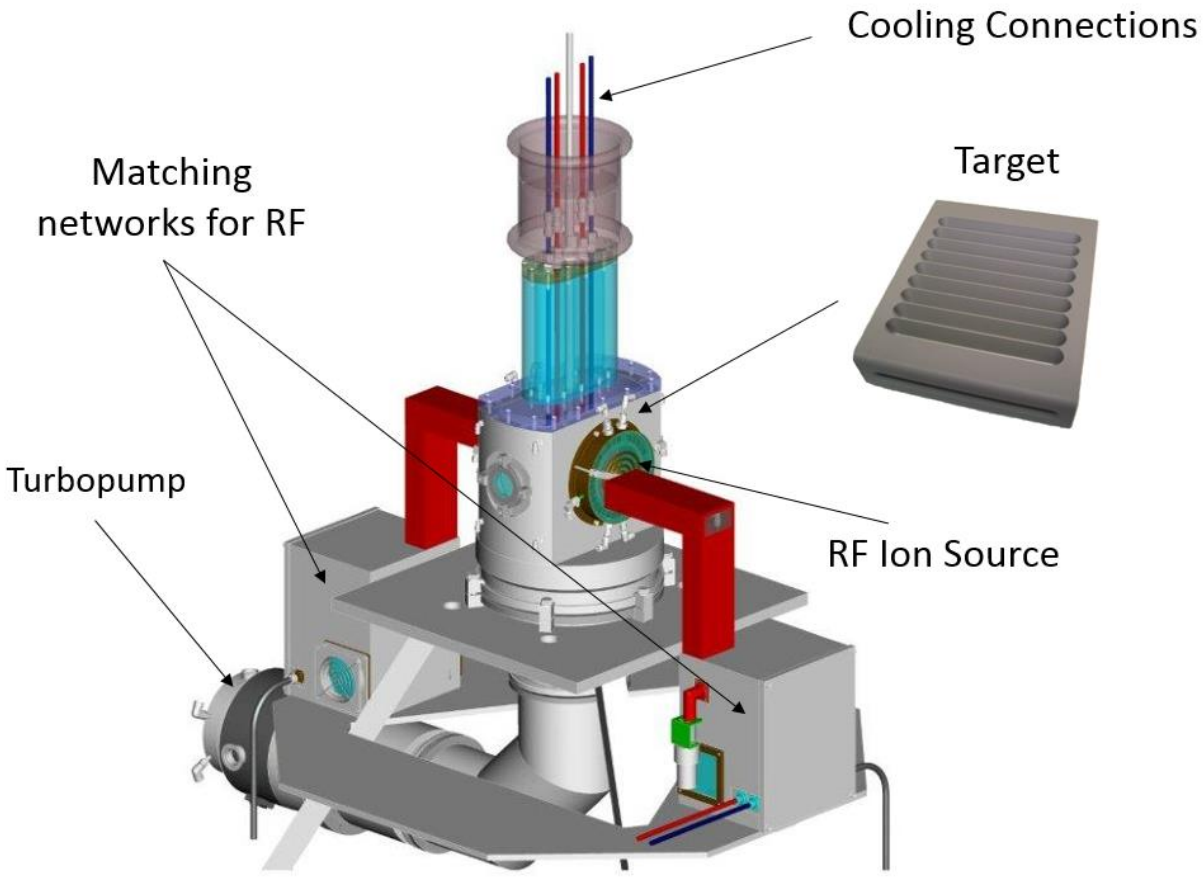

Figure 1.3. Schematic of HFNG taken from [11]

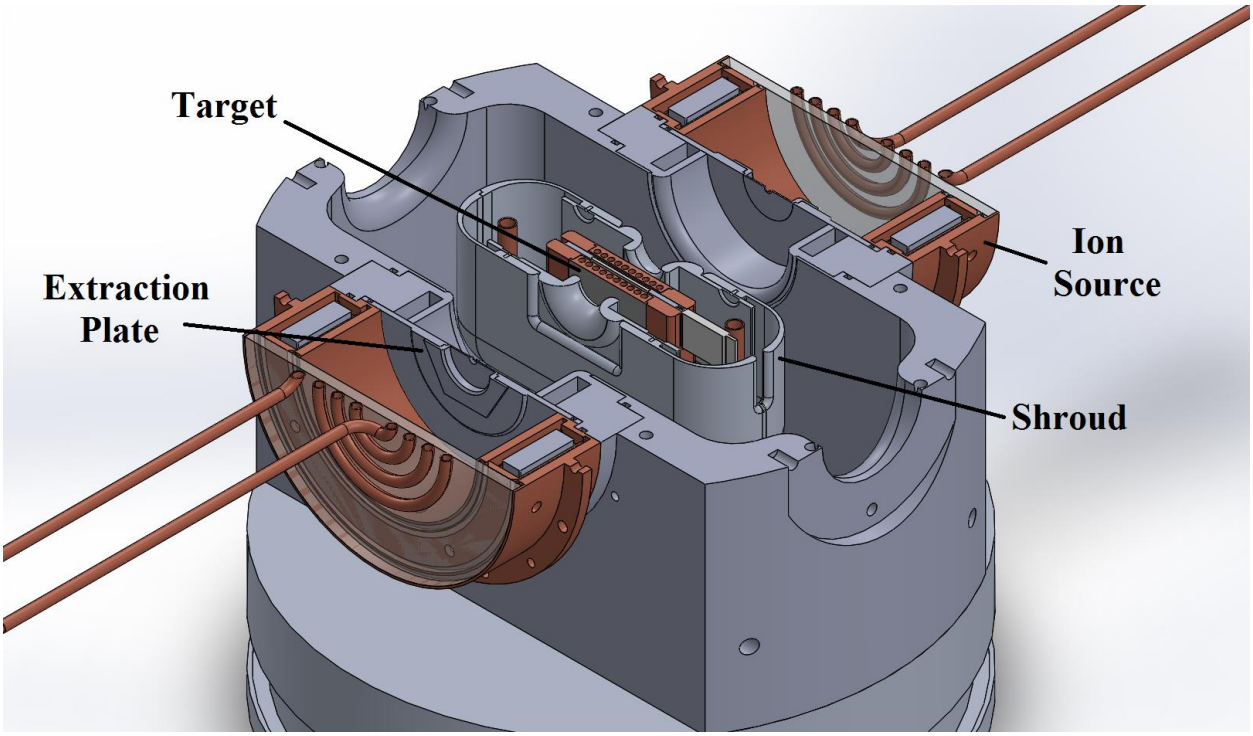

Figure 1.4. Inside view of HFNG, also taken from [11]

1.6 Neutron scattering

Neutrons scattering in materials can either be elastic or inelastic, depending on whether kinetic energy is conserved. In elastic scattering, kinetic energy and linear momentum are conserved: there is no change in internal energy of either the neutron or the scattering material. In the case of inelastic scattering, the scattering material is left in an excited state. In hydrogen and carbon, scattering is elastic at the energy of neutrons produced in HFNG since hydrogen has no excited state and the first excited state of carbon (4.4 MeV) is well above the maximum neutron energy in HFNG (2.78 MeV at deuteron energy of 100 keV). The first excited state of carbon is shown in Figure 1.5.

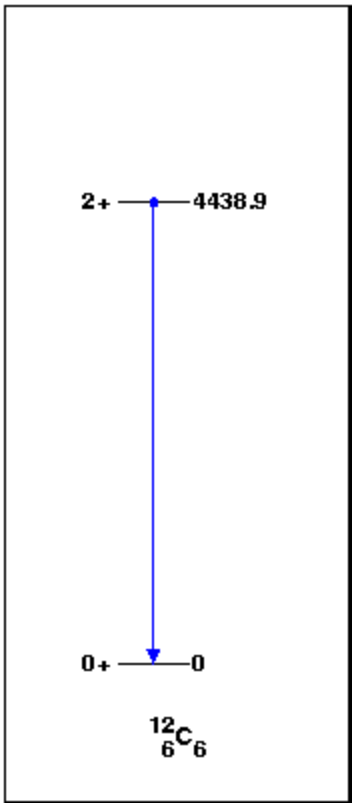

Figure 1.5. Ground and first excited states in ^{12}C. The energy is in keV [13]

Hydrogen has high thermal neutron elastic scattering cross section as shown in Figure 1.6.

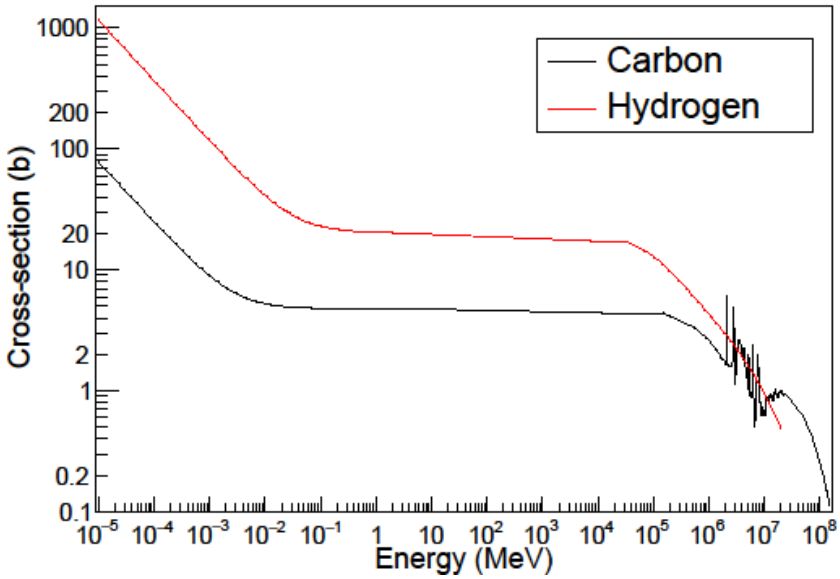

Figure 1.6. Elastic scattering cross-section of H and C taken from evaluated nuclear data [14]

The final energy, E' of neutrons in elastic scattering from atoms of mass A is given in [5] as:

$$\mathrm{E}' = \mathrm{E}\frac{\mathrm{A}^2 + 1 + 2\mathrm{A}\cos(\theta)}{(\mathrm{A}+1)^2} \tag{1.16}$$

Where θ is the scattering angle in the center-of-mass system, and E is the incident neutron energy.

A measure of how much energy neutrons lose on scattering elastically on an atom is the quantity described as logarithm of energy decrement:

$$\xi = \left(\log\frac{\mathrm{E}'}{\mathrm{E}}\right)_{\mathrm{avg}} = 1 + \frac{(\mathrm{A}-1)^2}{2\mathrm{A}}\,\mathrm{In}\frac{\mathrm{A}-1}{\mathrm{A}+1} \tag{1.17}$$

The average logarithm of energy decrement, ξ, is related to the number of collisions n [5], by:

$$\log\mathrm{E}'_{\mathrm{n}} = \log\mathrm{E} - \mathrm{n}\xi$$

Values of ξ , taken from [5], for atoms in a material of interest, polyethylene, is shown in Table 1.3:

Atom	ξ	E' (MeV)
H	1	1.02
C	0.158	2.37

Table 1.3. Average logarithm of energy decrement for H and C and neutron energies after one collision.

For HFNG, the maximum energy of neutrons is about 2.78 MeV. After one collision with the atoms of H and C in polythene the neutron energy is shown in Table 1.3. will be handy when we consider the two interactions of neutrons with indium that are of interest in characterizing the flux of thermal and fast neutron spectrum within the HFNG in the presence and absence of polyethylene plates.

Understanding the angular dependence of the neutron energy and yield makes it possible to build an MCNP input file.

2 Experiment and data analysis

2.1 The Set-up

In this chapter, a description of the experimental set-up and steps used in analyzing the experimental data are described.

Two sets of nine discs of natural indium foils were prepared for irradiation in the High Flux Neutron Generator (HFNG) at the Nuclear Engineering department of University of California Berkeley. The masses of the foils range from 0.0734 - 0.3074 g. An aluminum holder with polyethylene handle was used to hold the foil, Figure 2.1.

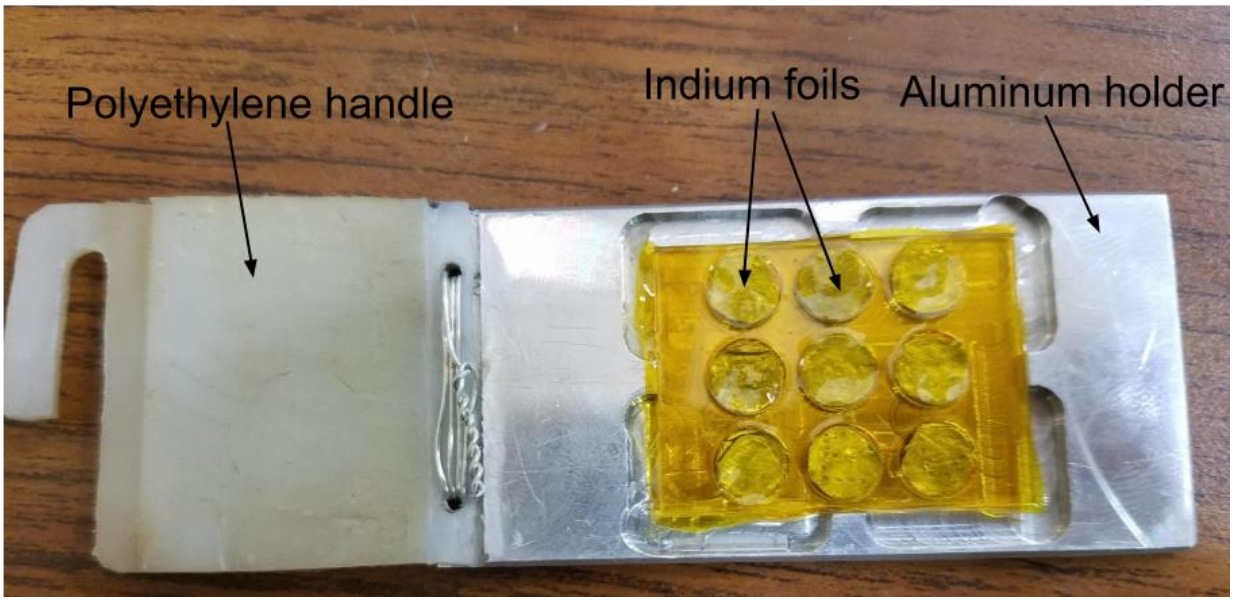

Figure 2.1. Indium foils in the holder.

The first set of indium foils were inserted in the HFNG chamber and 20 cm thick polyethylene was used to cover the chamber as shown in Figure 2.2. The foils were then irradiated for four hours. At the end of irradiation, the foils were left to ‘cool down’ for 30 minutes so that activation products with short half-lives could decay away, making it safe to enter the irradiation room to remove the foils.

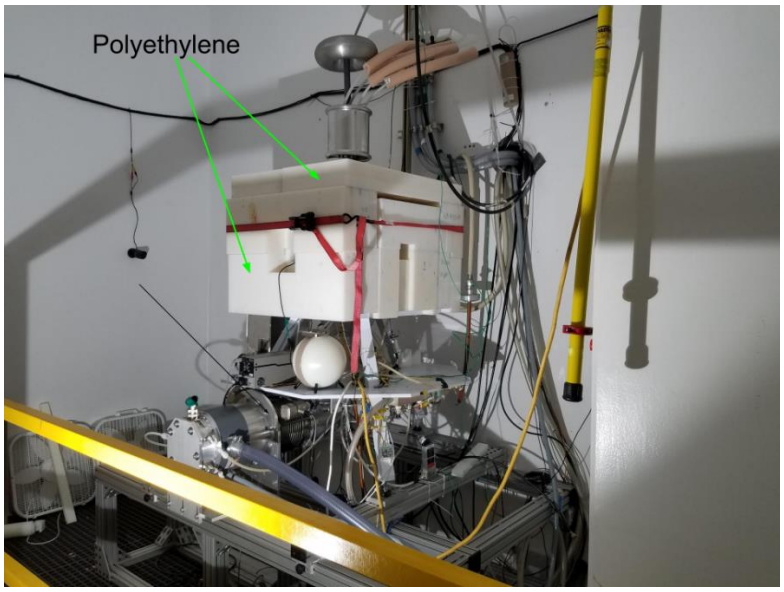

Figure 2.2 HFNG showing the polyethylene cover just before the first irradiation.

Counting was done using Ortec's High Purity Germanium detector, *Figure 2.3*.

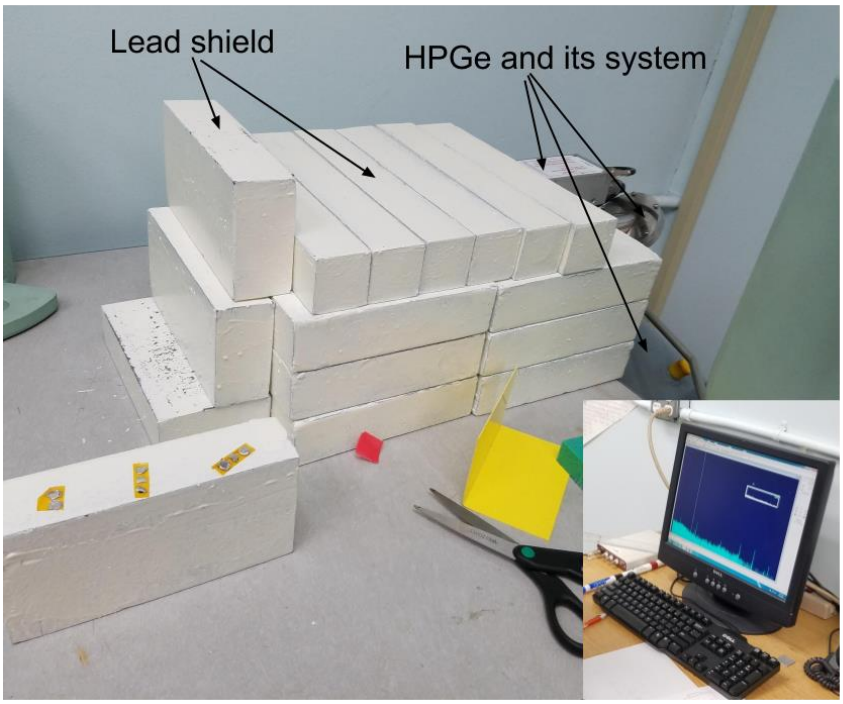

Figure 2.3. The HPGe detector. The lead plates are to reduce background radiation. Inset shows GammaVision acquiring gamma spectra.

While counting was being done, the second set of indium foils was irradiated, but without any polyethylene plates surrounding the chamber. The irradiation lasted

for four hours. By the time the irradiation was completed, the counting of the first set of foils was completed.

2.2 Detector energy and efficiency calibration

2.2.1 Detector energy calibration

The spectra from ^{152}Eu standard was used to calibrate the Gmmavision. A few hours to the start of the irradiation, spectra from ^{152}Eu was collected for about five hours. Some known ^{152}Eu spectra was identified together with their channel numbers as shown in

Table 2.1.

Energy (keV)	Channel number
121.78	153
244.7	309
344.28	435
778.9	985
964.08	1219
1085.87	1374
1112.07	1407
1408.01	1781

Table 2.1. ^{152}Eu energy and corresponding channel number.

Using ROOT [15] an object oriented data analysis framework, the data was fitted with a first order polynomial of the form:

$$E = 0.790x + 0.698 \qquad (2.1)$$

where E is energy in keV, and x is the channel number. Equation 1 enabled the conversion of channel number to energy value.

2.2.2 Detector efficiency calibration

For efficiency calibration, the same ^{152}Eu standard was used. This isotope has energies in the range of interest. At the time of calibration of the detector the activity of the ^{152}Eu was 39368 Bq. A few hours to the start of irradiation, counts at some well resolved prominent energies were taken for approximately five hours. The energies used and their branching ratio is shown in Table 2.2. Branching ratio values was got from [16].

Energy(keV)	Branching Ratio (%)
121.7	28.58
244.7	7.583
344.3	26.5
411.1	2.234
444	2.821
778.9	12.942
867	4.245
964.1	14.605
1085.9	10.207
1112.1	13.644
1299.1	1.623
1408	21.005

Table 2.2. Some ^{152}Eu energies and branching ratio used in efficiency calibration

To calculate the peak area, background was subtracted from the calibration spectrum shown in Figure 2.4. The implementation of Sensitive Nonlinear Iterative Peak (SNIP) clipping algorithm [17] in ROOT data analysis framework was used to remove the background.

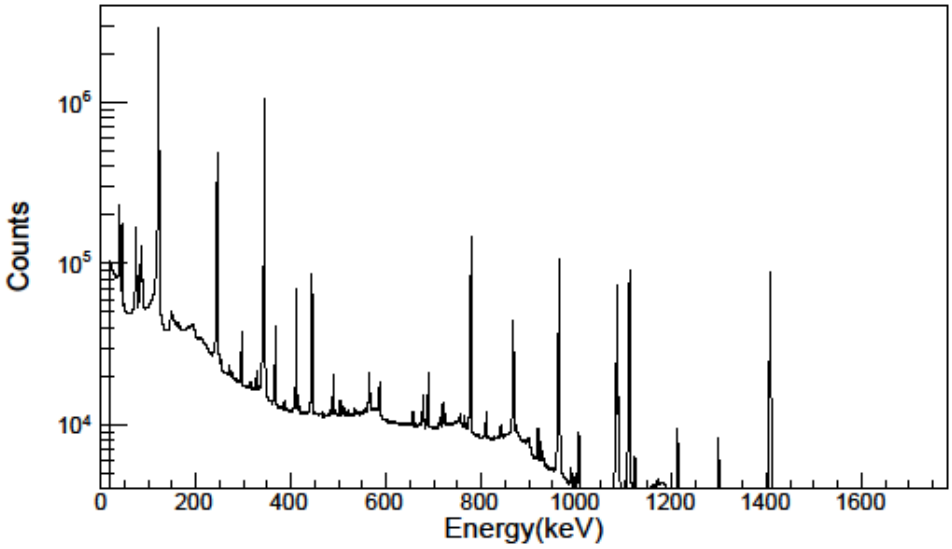

Figure 2.4. Calibration spectrum from ^{152}Eu

For each energy peak, a gaussian function was fitted. The function is of this form:

$$P_0 \exp\left(-0.5\left(\frac{x - P_1}{P_2}\right)^2\right) \quad (2.2)$$

Where P0, P1 and P2 are constants, and x is the energy. The net counts, which is the area of the gaussian, is calculated by integrating. Thus:

$$\text{Area} = \int_{-\infty}^{\infty} P_0 \exp\left(-0.5\left(\frac{x - P_1}{P_2}\right)^2\right) dx \quad (2.3)$$

$$\text{Net counts} = \text{Area} = P_0 \times P_2 \times \sqrt{2\pi} \quad (2.4)$$

Efficiency is calculated from:

$$\varepsilon = \frac{\text{number of photons detected in the energy peak in a given time}}{\text{number of photons in the energy peak emitted during the same time}} \quad (2.5)$$

The efficiency was plotted and fit with a function of the form:

$$\varepsilon = \exp(P_2 * \ln(x)^2 + P_1 * \ln(x) + P_0) \qquad (2.6)$$

graph of the efficiency is shown below:

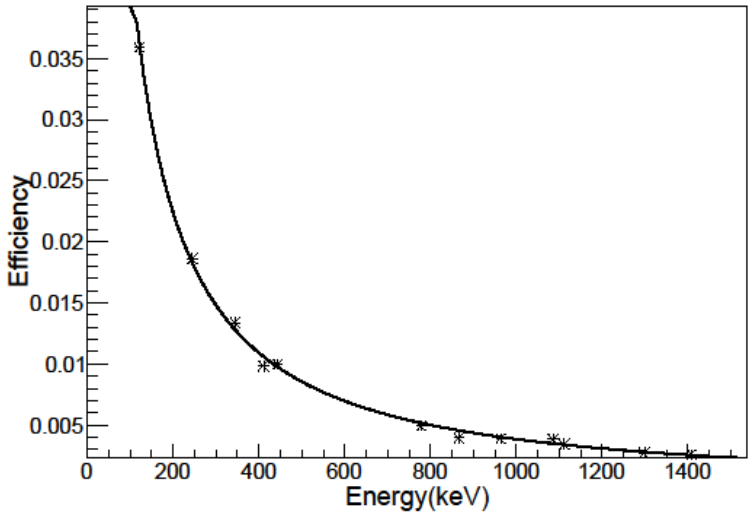

Figure 2.5. Efficiency plot

Figure 2.5 will enable the determination of the efficiency at the gamma energy of interest, in this care 336 and 417 keV

2.3 Curve fitting

After 4 hours irradiation, the foils were left to "cool down". The waiting time before removing the foil from the irradiation position was 30 minutes. Tables 3 and 4 gives the waiting time for individual foils and respective counting time.

foil	1	2	3	4	5	6	7	8	9
Waiting time(s)	2040	2460	2880	3240	3660	4080	4500	4860	5280
counting time(s)	300	300	300	300	300	300	300	300	300

Table 2.3. Waiting and counting time for presence of polyethylene blocks

foil	1	2	3	4	5	6	7	8	9
waiting time(s)	1920	2460	3000	3540	4080	4560	5040	5520	5760
counting time(s)	400	300	300	300	300	300	300	300	300

Table 2.4. Waiting and counting time for absence of polyethylene blocks

A high purity germanium (HPGe) was used to count each foil. The counting time was chosen so that a good statistic could be gotten for all the foils, taking note that the next foil to be counted always have lager waiting time which could affect the activity of the 54 minutes lived ^{116m1}In.

The spectrum of the central indium foil is given below in Figure 2.6.

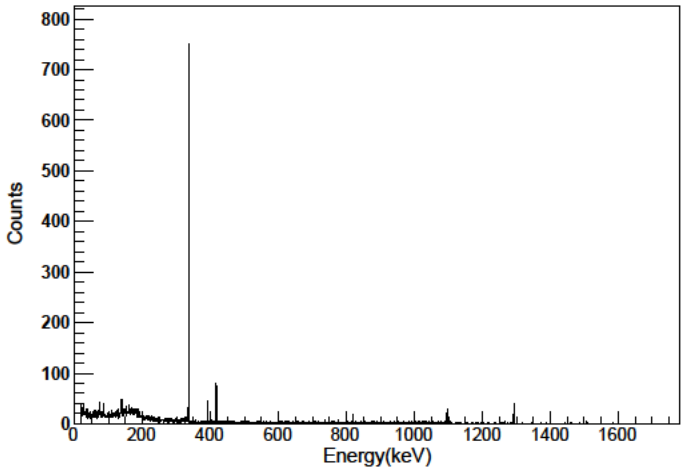

(a)

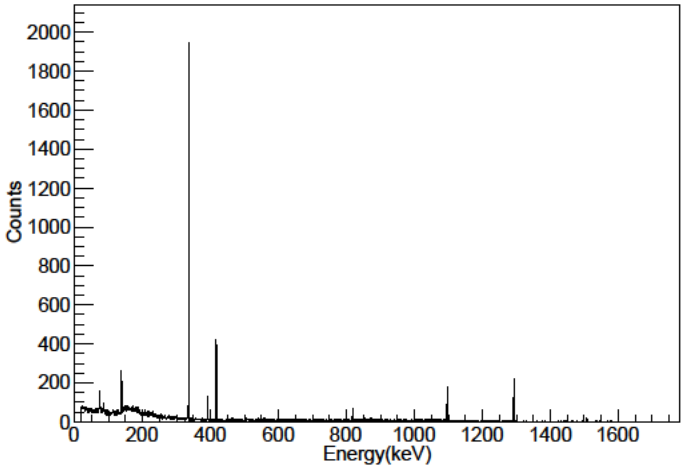

(b)

Figure 2.6. Spectrum from central indium foil. (a) no polyethylene plate cover. (b) polyethylene plate cover in position.

To get peak energy counts, background removal using Sensitive Nonlinear Iterative Peak (SNIP) clipping algorithm [17] implemented in ROOT data analysis software was again employed, Figure 2.7. Then a gaussian function was fitted to each energy peak of interest using TSpectrum class of ROOT data analysis software, and fit parameters were used to calculate the counts using Figure 2.4.

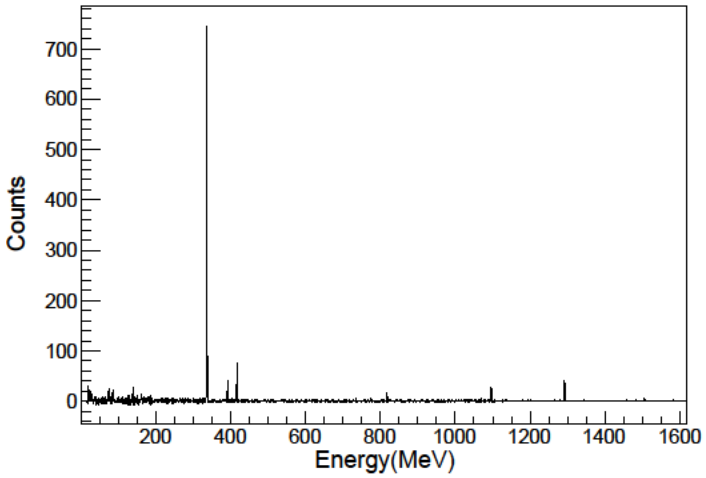

(a)

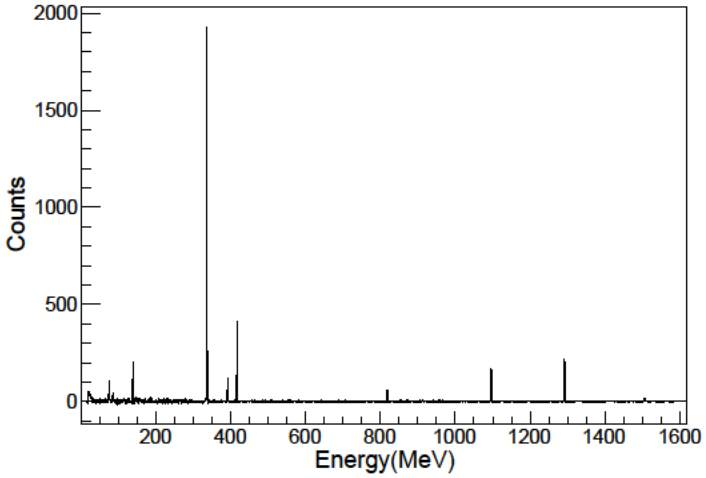

(b)

Figure 2.7. Background subtracted spectra of central foil. (a) no polyethylene plate covers. (b) polyethylene plate cover in place.

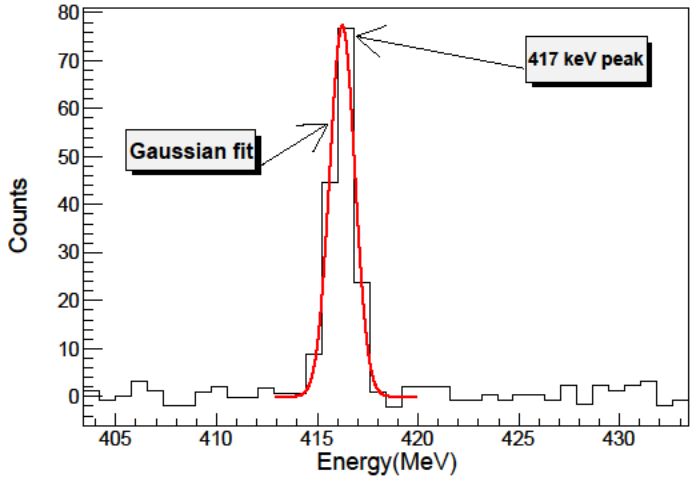

Figure 2.8. Fitting the peaks with Gaussian function to find the peak area(counts) of 417 keV peak.

336 keV		417 keV	
Counts	Error	Counts	Error
796.7389	40.77829	195.9063	15.72708
1504.91	66.55818	278.5924	23.48984
666.909	38.06511	116.7681	15.89214
1227.175	48.41182	185.0664	18.76779
1022.033	41.39449	128.8713	15.96619
1615.292	55.16076	187.7004	20.7164
1182.671	47.61482	166.7629	17.03822
657.0169	32.14434	83.83582	10.03378
1238.793	48.81982	135.5614	19.42233

Table 2.5. Counts from gaussian fits to peaks for absence of polyethylene plates.

336 keV		417 keV	
Counts	Error	Counts	Error
570.6096	32.54508	460.0211	28.21964
1441.824	54.15005	596.5216	28.45173
980.1219	40.83081	489.6847	28.22684
844.1982	40.73941	386.3084	29.53428
2618.134	64.28726	597.9134	34.83683
1498.828	56.29603	420.692	28.49434
567.1161	29.15296	306.539	23.6875
868.4994	40.59518	277.9162	22.76367
590.4497	15.32597	213.7462	19.17473

Table 2.6. Counts from gaussian fits to peaks for presence of polyethylene plates.

The ratio of ^{116m1}In rate of reaction for presence and absence of the polyethylene plates is shown in Table 2.7.

Foil	Rate Ratio	Error
1	3.82	0.386
2	2.39	0.232
3	3.18	0.470
4	3.59	0.456
5	1.78	0.244
6	2.19	0.283
7	3.58	0.459
8	2.63	0.382
9	2.87	0.486

Table 2.7. The ratio of ^{116m1}In for when polyethylene plate is present and when absent.

2.4 Data analysis

2.4.1 Production and decay of radioactivity

When a radioactive isotope is being produced in a nuclear reaction, for instance in nuclear reactor, the isotope also decays. The amount of the radioactive

isotope at any time t depends on its production rate R and rate of disintegration A. Let j be the radioactive atom:

$$dN_j = R_j dt - A dt \tag{2.7}$$

Equation 2.7 is the atom balance equation. It could be re-written using the fact that $A = N_j \lambda_j$, as:

$$\frac{dN_j}{dt} = R_j - \lambda_j \tag{2.8}$$

This is a first order linear differential equation whose solution yields the concentration of atom N_j at any given time as:

$$N_j = \frac{R_j}{\lambda_j}\left(1 - \exp(-\lambda_j t)\right)$$

The number of atoms of isotope j at the end of irradiation time $t = t_i$ is:

$$N_{j1} = \frac{R_j}{\lambda_j}\left(1 - \exp(-\lambda_j t_i)\right) \tag{2.9}$$

After irradiation, N_{j1}decays exponentially. Thus, for a cooling time t_d, the number of N_{j2} remaining is given by

$$N_{j2} = N_{j1} \times \exp(-\lambda_i t_d) = \frac{R_j}{\lambda_j}\left(1 - \exp(-\lambda_j t_i)\right) \times \exp(-\lambda_i t_d)$$

If the number of either 316 keV or 416 keV gamma ray emitted by the atom is counted for a time t_c, the number observed is given by:

$$N_{j3} = N_{j2}\left(1 - \exp(-\lambda_j t_c)\right)$$
$$= \frac{R_j}{\lambda_j}\left(1 - \exp(-\lambda_j t_i)\right) \times \exp(-\lambda_i t_d) \times \left(1 - \exp(-\lambda_j t_c)\right)$$

Since not every decay result in emission of the gamma ray of interest and not every gamma ray emitted by the atoms are detected by the detector, the number of counts is therefore given as:

$$N_\gamma = N_{j3} \times B.R_j \times \epsilon$$

Where B.R is the branching ratio of the gamma ray and ϵ is the absolute full-energy peak efficiency of the detector for the gamma ray.

$$\therefore N_\gamma = \frac{R_j}{\lambda_j}\left(1 - \exp\left(-\lambda_j t_i\right)\right) \times \exp(-\lambda_i t_d) \times \left(1 - \exp\left(-\lambda_j t_c\right)\right) \times B.R_j \times \epsilon \quad (2.10)$$

2.5 Quadratic surface fit to determine the center of foil

Because the center of the foils may not coincide with the neutron production point, a quadratic surface fit was performed to determine the center. Also, the uncertainty in alignment is the major source of systematic uncertainty. The result was used in the MCNP simulation to ensure that the simulation is done under the same geometric configuration of the experiment.

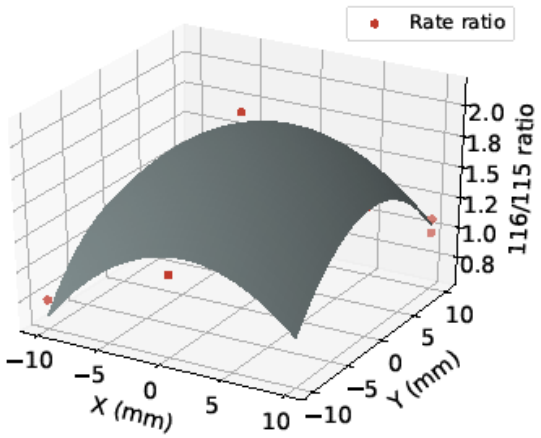

Figure 2.9. Quadratic surface fit to count data. The central indium foil is displaced from the axis by x, y value of 1.33 mm and 0.5 mm respectively.

3 The simulation

3.1 Structure of MCNP input file

The input file is shown in Appendix A. The original input was prepared by a former student who worked on the design of the HFNG. A two-dimensional MCNP rendering of the geometry of the generator is shown in Figures 3.1, 3.2 and 3.3.

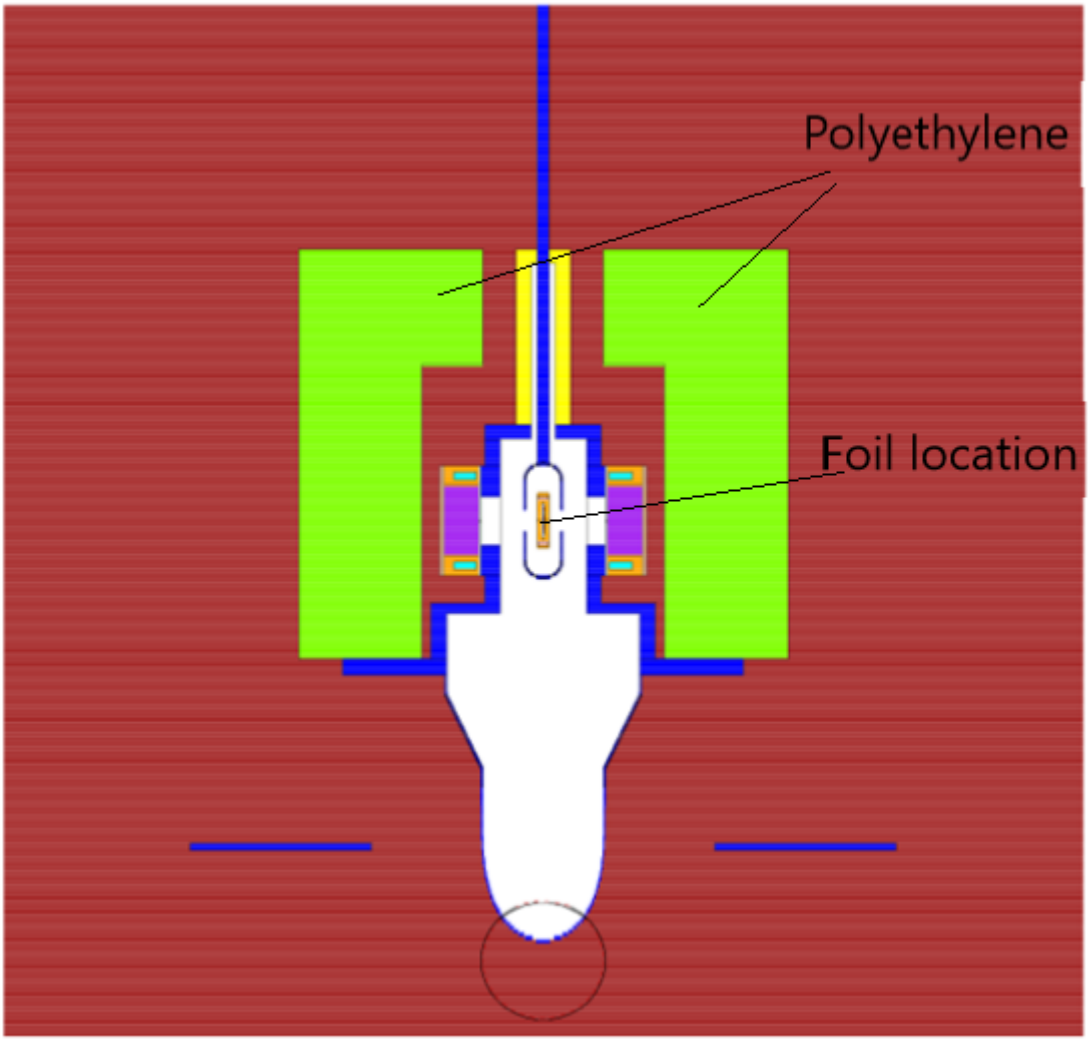

Figure 3.1. Side view of the HFNG showing the polyethylene cover (green).

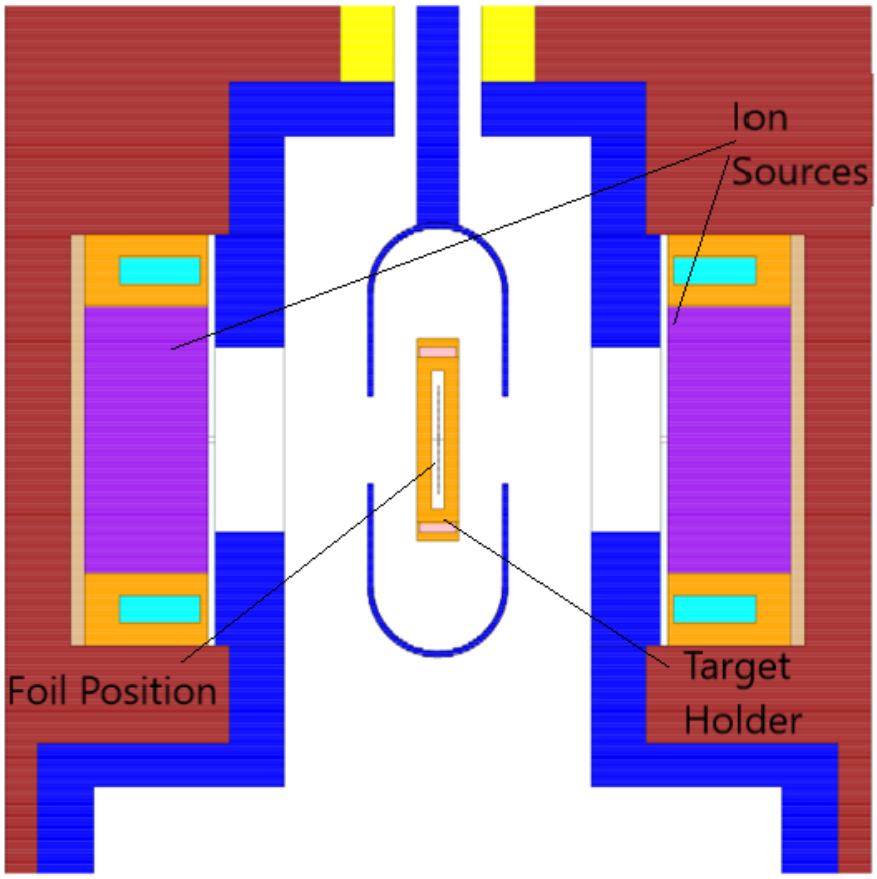

Figure 3.2. Side view of the HFNG showing the shroud, ion source and target.

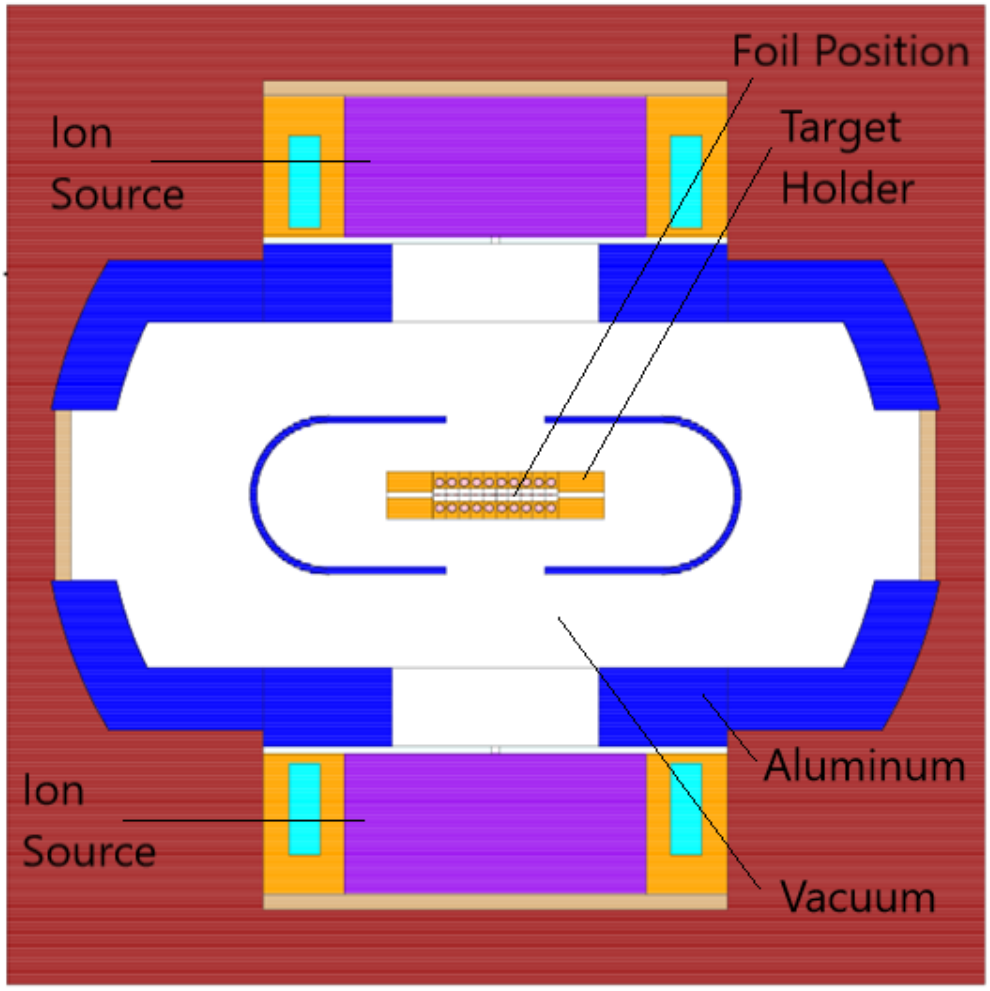

Figure 3.3. 2D top view of HFNG chamber in MCNP

3.2 Theory of the simulation

The simulation is divided into two: the first part deals with the simulation of rates of inelastic scattering into the ^{115m}In metastable state and radiative capture into the ^{116m1}In metastable state in the absence of polyethylene plates cover. The second simulation is like the first except that polyethylene plates, as shown in Figure 3.1, are used to surround the HFNG chamber. The ^{115m}In and ^{116m1}In decay by emission of 336.2 keV and 127.3 keV gamma rays respectively. Using these rates, evaluated data can be compared to experiment.

Primary neutrons produced in the HFNG interact with ^{115}In in two ways: inelastic scattering in which the indium atom is left in a metastable state ^{115m}In and radiative capture reaction in which the indium atom captures a neutron and de-excite

either to the ground state or to metastable states ^{116m1}In and ^{116m2}In. It is the metastable state ^{116m1} that is of interest in this work

Primary neutrons from the HFNG scatter inelastically in ^{115}In, forming ^{115m}In:

$$^{115}_{49}\mathrm{In} + \mathrm{n} \rightarrow {}^{115\mathrm{m}}_{49}\mathrm{In} + \mathrm{n}' \qquad (3.1)$$

This inelastic scattering into the metastable state is a threshold reaction, with a threshold energy of about 340 keV. The cross section for the inelastic interaction of the neutron with ^{115}In is given in Figure 3.4. This cross section has its maximum around 2.5 MeV which, incidentally, is the average energy of neutrons emitted in the d(d,n) reaction.

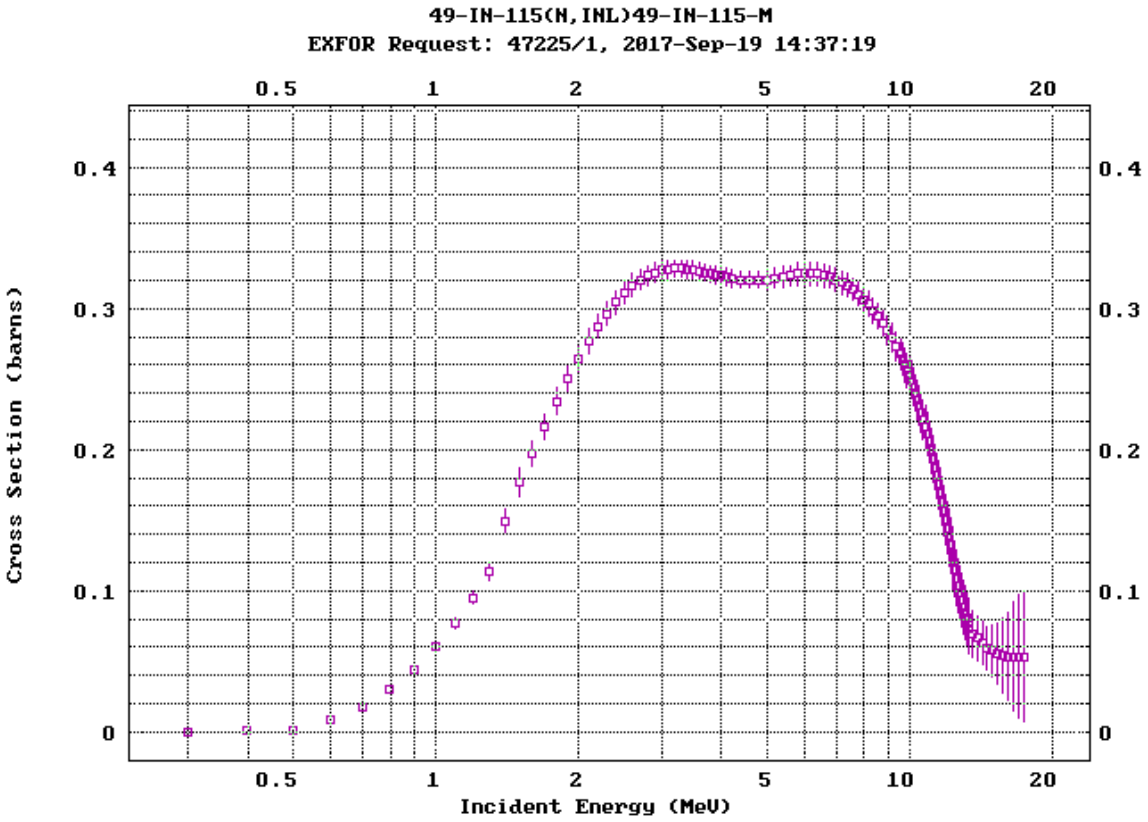

Figure 3.4. Cross-section for inelastic scattering of neutron in ^{115}In. The figure is taken from Nuclear Reaction Experimental Data, alias EXFOR [18].

The ^{115m}In has a half-life of 4.49 hours and decays 95% of the time to the ground state of indium by internal conversion and 5% into $^{115}_{50}$Sn by beta decay [16]. The internal conversion gives rise to the characteristic 336 keV gamma ray which is

used in counting the number of $^{115}_{49}\mathrm{In}$ produced when natural indium is exposed to the primary neutrons from the HFNG.

Radiative capture into the 127.3 keV metastable state in $^{116}\mathrm{In}$, producing $^{116m1}\mathrm{In}$, proceeds through formation of compound nucleus.

$$^{115}_{49}\mathrm{In} + \mathrm{n} \rightarrow {}^{116}_{49}\mathrm{In}^{*} \qquad (3.2)$$

the cross section is shown in Figure 3.5.

The $^{116}\mathrm{In}$* de-excites to $^{116m1}\mathrm{In}$, $^{116m2}\mathrm{In}$ and $^{116}\mathrm{In}$ states with respective half-lives of 54.29 minutes, 2.18 seconds and 14.10 seconds [16]. The $^{116m2}\mathrm{In}$ decays to $^{116m1}\mathrm{In}$ 100% of the time. However, the de-excitation channel that is of interest in this work is the

$$^{116}_{49}\mathrm{In}^{*} \rightarrow {}^{116m1}_{49}\mathrm{In} + \gamma$$

channel. The sum of branching ratio for the production of the two metastable states is 0.79 at thermal neutron energy as given in ENDF/B-VII.1 nuclear data [19] retrieved from [20] as given by [21]. Thus, the cross section in Figure 3.5 may need to be scaled by 0.79.

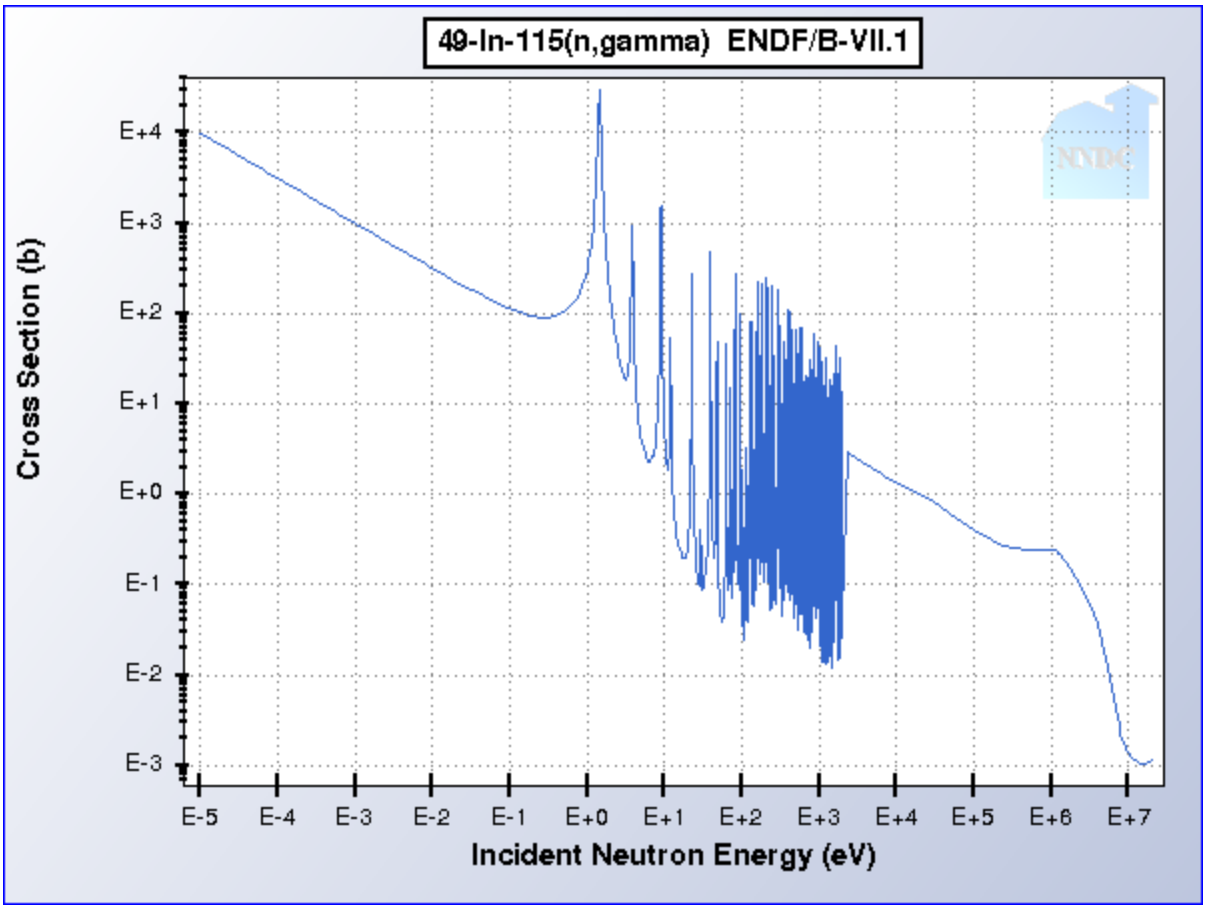

Figure 3.5. Cross-section for radiative capture in ^{116}In. Taken from Evaluated Nuclear Data Library, ENDF/B-VII.I [20].

When neutron of flux ϕ passes through a given isotope, the rate of interaction R in reaction/s/unit volume is given by:

$$R = \int N\phi(E)\sigma(E)dE \qquad (3.3)$$

Where
N is the atom density of the isotope in (atoms/cm^3).
$\phi(E)$ is the energy dependent flux (in neutrons/cm^2-s).
$\sigma(E)$ is the energy dependent neutron cross-section of the isotope (in cm^2).
In MCNP calculation, (3.3) is normalized by the number of neutrons simulated and is equivalent to

$$R_{MCNP} = \frac{1}{N}\int \phi(E)\sigma(E)dE \qquad (3.4)$$

Where N is the number of neutrons simulated.

If we thus multiply (3.4) by number of neutrons produced in the deuteron reaction per second we then get the reaction rate R. In other words:

$$R = R_{MCNP} \times \text{neutron current}$$

If the volume of target (foil) is V, then we have:

$$R_{MCNP} = C \times V \int \phi(E)\sigma(E)dE \qquad (3.5)$$

The foils are mostly in form of discs with radius of 0.495 cm and average thickness of 0.05cm.

The term R_{MCNP} is what the MCNP FMESH tally and an FM multiplier calculates. The FM multiplier card simply tells the code to pull a given cross section and use it in (3.5).

3.3 Results from simulation

A billion neutrons were simulated on the Berkeley Research Computing supercomputer cluster using 24 core processor. It took about two and half days to finish running the simulation. A python script, see Appendix B, was used to extract the output and calculate ratios of rates of reaction for later use.

Foil	polyethylene/no polyethylene	Error
1	5.932	0.269
2	5.161	0.236
3	6.404	0.345
4	4.673	0.188
5	3.420	0.102
6	4.789	0.216
7	5.800	0.257
8	4.800	0.236
9	6.489	0.395

Table 3.1. Rate ratios, representing rate of reaction for formation of ^{116m1}In the presence and absence of polyethylene plate covers, at different Indium foil position.

Foil	Rate ratio	Error
1	2.172	0.073
2	2.554	0.065
3	1.833	0.074
4	2.732	0.128
5	3.552	0.049
6	2.228	0.081
7	2.183	0.086
8	2.603	0.077
9	2.077	0.071

Table 3.2. Ratios of rate of ^{115m}In to ^{116m1}In production at different indium foil positions in the absence of polyethylene cover.

Foil	Rate ratio	Error
1	0.344	0.007
2	0.495	0.008
3	0.276	0.006
4	0.580	0.013
5	1.018	0.019
6	0.475	0.009
7	0.396	0.008
8	0.557	0.010
9	0.308	0.006

Table 3.3. Ratios of rate of ^{115m}In to ^{116m1}In production at different indium foil positions in the presence of polyethylene cover.

Foil	Value	Error
1	5.922	0.267
2	5.154	0.236
3	6.392	0.346
4	4.675	0.187
5	3.419	0.103
6	4.794	0.217
7	5.789	0.253
8	4.794	0.233
9	6.476	0.399

Table 3.4. Ratio of second column in Table 3.2 to second column in Table 3.3.

4 Validation of Polyethylene Nuclear Data

4.1 Introduction

Validation of the nuclear data for carbon and hydrogen in polyethylene will be done using two different approaches: single ratio method and double ratio method. In the first case, the ratio of ^{116m1}In reaction rate taken in the presence and absence of polyethylene plates cover is compared between experiment and simulation. In the second case, a double ratio in which the ratio of ^{115m}In to ^{116m1}In reaction rates is first taken for the absence of poly and then in the presence of poly. Another ratio of the above resulting ratios is then taken. This ratio is essentially the ratio in the first method. In this method, use is made of the fact that ^{115m}In formation is a threshold reaction and that neutrons scattered by the neutron generator structures essentially have their energies below the threshold of ^{115m}In formation. Thus, presence of polyethylene plates doesn't make any practical difference in the ^{115m}In reaction rate. As a result, taking the ratio of the first ratio cancels out the ^{115m}In reaction rate.

The first approach has many advantages. One, calculation of efficiency is not required since efficiency term cancels out. Two, branching ratios also cancel out. Therefore, uncertainties from efficiency and branching ratio varnishes. In the second approach, the mass of indium foils cancels out, so does the uncertainty in foil mass measurement.

The nine indium foils and their relative position is shown in Figure *4.1*

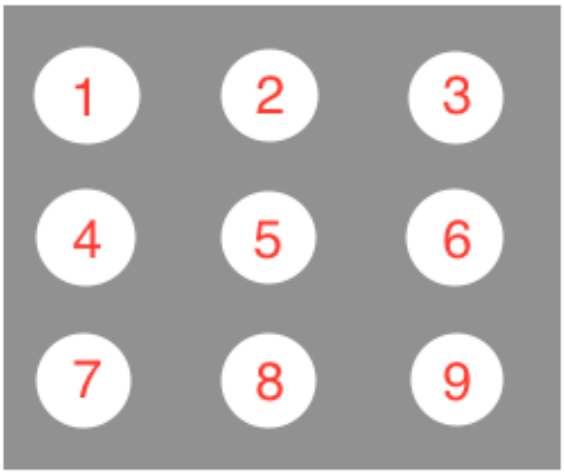

Figure 4.1. Nine indium foils. Foil 5 is at the origin. The z-axis, defined by the direction of the deuteron beam, passes through the center of foil 5 perpendicular to the plane.

The indium foils have a center-to-center spacing of 1 cm, while the perpendicular distance between the point where deuteron fusions are occurring (i.e. the neutron production site) and the foil plane is 1 cm.

4.2 Comparison of the ratio of ^{116m1}In between experiment and simulation.

$^{116m1}_{49}$In is a metastable state of $^{116}_{49}$In. It decays by beta emission to ^{116}Sn with branching ration of 100%. The ^{116}Sn is left in excited state and emits a gamma ray cascade. The last gamma ray in the cascade is the 416 keV line with intensity of 27% [13].

Using equation 2.10, the number of the 416 keV gamma rays detected after counting for a time t_c is:

$$N_{416\,keV} = \frac{R_{116m1}}{\lambda_{116m1}}(1-\exp(-\lambda_{116m1}t_i)) \times \exp(-\lambda_{116m1}t_d) \times (1-\exp(-\lambda_{116m1}t_c)) \times B.R._{116m1} \times \epsilon \quad (4.1)$$

And thus

$$R_{116m1} = \frac{N_{416\,keV} \times \lambda_{116m1}}{(1-\exp(-\lambda_{116m1}t_i)) \times \exp(-\lambda_{116m1}t_d)} \times \frac{1}{(1-\exp(-\lambda_{116m1}t_c)) \times B.R_{116m1} \times \epsilon_{416\,keV}} \quad (4.2)$$

Taking the ratio of the equation above for the presence of polyethylene plane and absence of polyethylene plate cover and noting that irradiation time is the same, gives:

$$\frac{R_{Poly}}{R_{no\ poly}} = \frac{N_{Poly} \times \exp(-\lambda t_{d,no\ poly})}{N_{no\ poly} \times \exp(-\lambda t_{d,poly})} \times \frac{(1-\exp(\lambda t_{c,no\ poly}))}{(1-\exp(\lambda t_{c,poly}))} \quad (4.3)$$

Thus, the ratio of counts is to be multiplied by two factors: waiting factor, counting factor and counting factor. Their values for each foil are shown in Table 4.1.

Foil	Waiting factor	Counting factor
1	1.026	1.319
2	1.000	1.000
3	0.975	1.000
4	0.938	1.000
5	0.914	1.000
6	0.903	1.000
7	0.891	1.000
8	0.869	1.000
9	0.903	1.000

Table 4.1. Values of the multiplicative factors for each foil.

Before the experiment value can be compared to the value from simulation, equation 4.3 needs to be normalized to the respective mass of the indium foil and the deuteron beam currents.

Therefore, two more factors need to be multiplied to equation 4.3. They are: $\frac{m_{foil,no\ poly}}{m_{foil,poly}}$ and $\frac{I_{poly}}{I_{no\ poly}}$. The average deuteron current for the first experiment in which there are polyethylene plates surrounding the neutron generator was 8.2 mA, while that for the second experiment in which there is no polyethylene plates surrounding the neutron generator was 15.1 mA. Table 4.2 shows the normalization factors.

Foil	Mass factor	Deuteron beam factors
1	1.204	1.8
2	1.117	1.8
3	0.775	1.8
4	1.835	1.8
5	0.419	1.8
6	1.078	1.8
7	2.185	1.8
8	0.913	1.8
9	2.018	1.8

Table 4.2. Factor for normalizing the ratio of reaction rates so it can be compared to simulation.

Foil	Normalized ratio	Error
1	6.89	0.49
2	4.31	0.43
3	5.72	0.63
4	6.47	0.35
5	3.21	0.19
6	3.94	0.40
7	6.44	0.47
8	4.74	0.43
9	5.17	0.72

Table 4.3. Normalized ratios

Taking the rate ratios of experiment and simulation, Table 4.4 below is obtained.

Foil	Simulation/Experiment	Error
1	0.86	0.07
2	1.20	0.13
3	1.12	0.14
4	0.72	0.05
5	1.06	0.07
6	1.22	0.13
7	0.90	0.08
8	1.01	0.10
9	1.25	0.19

Table 4.4. Simulation to experimental ratio of ^{116m1}In reaction.

A plot of the ratio $\frac{R_{116m1,poly}}{R_{116m1,no\ poly}}$ is shown in Figure 4.2.

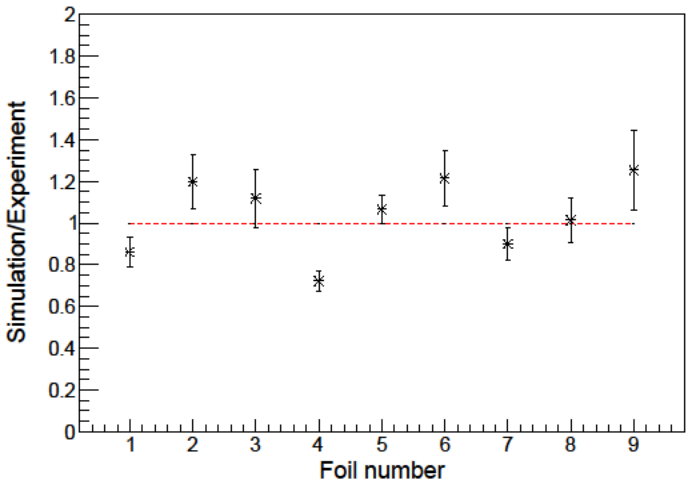

Figure 4.2 Comparison between simulation and experiment. The error bar is that of statistical error.

From Figure 4.2, the simulation to experiment ratio approaches the expected value of unity. That for the central indium foil, that is foil 5, agrees with the expected value of unity within limit of statistical error. Those of other foils have values near unity. This might be due to error in the modelling of the angular distribution of the neutron produced in the HFNG. Angular distribution data from [9] was given at 100 and 150

keV. Interpolation had to be used to get the value at 105 keV which is the accelerating voltage used in the experiment.

4.3 Comparison between experiment and simulation using ^{115m}In and ^{116m1}In double ratio method.

$^{115m}_{49}$In is a metastable first excited state of ^{115}In with energy of 336.24 keV and spin-parity of 1/2$^-$. It decays to the ground state by gamma ray emission and beta decay with branching ratio of 95% and 5% respectively [9]. The emitted gamma ray has energy of 336 keV. By calculating the expected number of 336 keV gammas after irradiation, cooling and counting, the simulation could be compared to experiment.

In competition with gamma ray emission is internal conversion, with an internal conversion coefficient of 1.073 [11]. This implies a probability of gamma ray emission per decay of $^{115m}_{49}$In as 45.83%.

Using equation 2.10, the number of the 416 keV gammas detected after counting for a time t_c is:

$$N_{416\,keV} = \frac{R_{116m1}}{\lambda_{116m1}}(1-\exp(-\lambda_{116m1}t_i)) \times \exp(-\lambda_{116m1}t_d) \times (1-\exp(\lambda_{116m1}t_c)) \times B.R._{116m1} \times \epsilon \quad (4.4)$$

And thus

$$R_{116m1} = \frac{N_{416\,keV} \times \lambda_{116m1}}{(1-\exp(-\lambda_{116m1}t_i)) \times \exp(-\lambda_{116m1}t_d)} \times \frac{1}{(1-\exp(\lambda_{116m1}t_c)) \times B.R._{116m1} \times \epsilon_{416\,keV}} \quad (4.5)$$

Also from the same equation 2.10, the number of the 336 keV gammas detected after counting for a time t_c is:

$$N_{336\,keV} = \frac{R_{115m}}{\lambda_{115m}}(1-\exp(-\lambda_{115m}t_i)) \times \exp(-\lambda_{115m}t_d) \times (1-\exp(\lambda_{115m}t_c)) \times B.R._{115m} \times \epsilon \quad (4.6)$$

And thus

$$R_{115m} = \frac{N_{336\,keV} \times \lambda_{115m}}{(1 - \exp(-\lambda_{115m} t_i)) \times \exp(-\lambda_{115m} t_d) \times (1 - \exp(\lambda_{115m} t_c))} \times \frac{1}{B.R_{115m} \times \epsilon_{336\,keV}} \quad (4.7)$$

Noting that the irradiation time is the same, the ratio of the reaction rates for ^{115m}In and ^{116m1}In is therefore given as

$$\frac{R_{115m}}{R_{116m1}} = \frac{N_{336\,keV} \times \lambda_{115m} \times \exp(-\lambda_{116m1} t_d)}{N_{416\,keV} \times \lambda_{116m1} \times \exp(-\lambda_{115m} t_d)} \times \frac{(1 - \exp(\lambda_{116m1} t_c)) \times B.R._{116m1} \times \epsilon_{416\,keV}}{(1 - \exp(\lambda_{115m} t_c)) \times B.R._{115m} \times \epsilon_{336\,keV}} \quad (4.8)$$

Thus, the ratio of counts is to be multiplied by five factors: the decay constant factor, the waiting time factor, the counting time factor, the branching ratio factor and the energy efficiency factor. These factors are shown in Table 4.5 for absence of polyethylene plates and Table 4.6. for when polyethylene plates are present.

Foil	Decay constant factor	Waiting factor	Counting factor	Branching ratio	Efficiency factor
1	0.202	0.722	4.794	0.604	0.786
2	0.202	0.658	4.834	0.604	0.786
3	0.202	0.601	4.834	0.604	0.786
4	0.202	0.548	4.834	0.604	0.786
5	0.202	0.500	4.834	0.604	0.786
6	0.202	0.461	4.834	0.604	0.786
7	0.202	0.425	4.834	0.604	0.786
8	0.202	0.392	4.834	0.604	0.786
9	0.202	0.376	4.834	0.604	0.786

Table 4.5. Values of factors in equation 4.8 for each foil with no polyethylene plates.

Foil	Decay constant factor	Waiting factor	Counting factor	Branching Ratio factor	Efficiency factor
1	0.202	0.707	4.834	0.604	0.786
2	0.202	0.658	4.834	0.604	0.786
3	0.202	0.613	4.834	0.604	0.786
4	0.202	0.577	4.834	0.604	0.786
5	0.202	0.537	4.834	0.604	0.786
6	0.202	0.500	4.834	0.604	0.786
7	0.202	0.466	4.834	0.604	0.786
8	0.202	0.438	4.834	0.604	0.786
9	0.202	0.408	4.834	0.604	0.786

Table 4.6. Values of factors in equation 4.8 for each foil with polyethylene plates are present.

Using the factors in Table 4.5 and counts in Table 2.5, the ratio $\frac{R_{115m}}{R_{116m1}}$ for the absence of polyethylene plates is shown in Table 4.7. Similarly, using the factors in Table 4.6 and the counts in Table 2.6, the ratio $\frac{R_{115m}}{R_{116m1}}$ for the presence of polyethylene plates is shown Table 4.8.

Foil	$\frac{R_{115m}}{R_{116m1}}$	Error
1	2.79	0.29
2	3.41	0.32
3	3.29	0.48
4	3.48	0.38
5	3.80	0.49
6	3.80	0.44
7	2.88	0.32
8	2.94	0.38
9	3.29	0.49

Table 4.7. Ratio of R_{115m} to R_{116m1} for absence of polyethylene.

Foil	$\frac{R_{115m}}{R_{116m1}}$	Error
1	0.84	0.07
2	1.52	0.09
3	1.18	0.08
4	1.21	0.11
5	2.25	0.14
6	1.71	0.13
7	0.82	0.08
8	1.31	0.12
9	1.08	0.11

Table 4.8. Ratio of R_{115m} to R_{116m1} for presence of polyethylene plates.

Taking the ratio of $\frac{R_{115m}}{R_{116m1}}$ in the absence of polyethylene plate and presence of polyethylene plates using values in Table 4.7 and Table 4.8 gives:

Foil	$\frac{R_{115m}}{R_{116m1}}\,\frac{\text{nopoly}}{\text{poly}}$	Error
1	3.32	0.42
2	2.24	0.25
3	2.80	0.46
4	2.88	0.41
5	1.69	0.24
6	2.23	0.31
7	3.49	0.50
8	2.24	0.36
9	3.05	0.54

Table 4.9. The double ratio of the two indium reaction rates

Before the experimental result can compare with simulation it needs to be normalized to the deuteron beam current. The average deuteron beams current for the first experiment in which there are polyethylene plates surrounding the neutron generator was 8.2 mA, while that for the second experiment in which there is no polyethylene plates surrounding the neutron generator was 15.1 mA. Thus, the normalizing factor is 1.8. Multiplying the second column in

Table 4.9 by 1.8 and taking the ratio of the result from the MCNP simulation (column 2 of Table 3.4) to this result, i.e. the experimental value, gives the result in Table 4.10.

Foil	Ratio	Error
1	0.99	0.13
2	1.28	0.16
3	1.27	0.22
4	0.90	0.13
5	1.12	0.17
6	1.20	0.18
7	0.92	0.14
8	1.19	0.20
9	1.18	0.22

Table 4.10. Simulation to experiment ratio of the double ratio method.

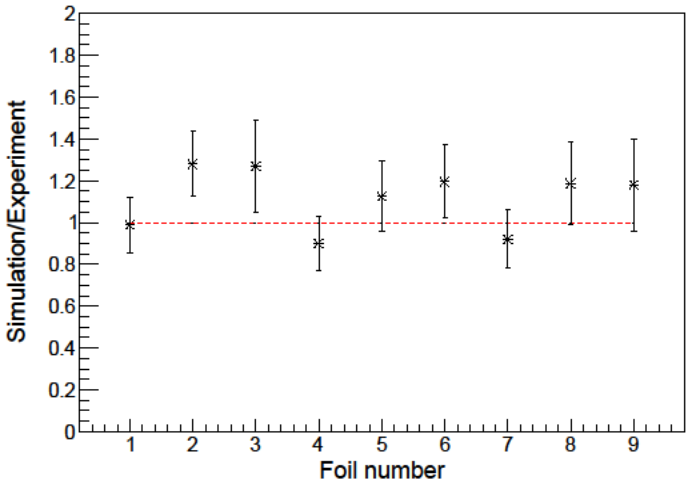

Figure 4.3 Comparison between simulation and experiment.

4.4 Systematic error

The major source of systematic error was the alignment of the plastic foil holder in such a way that the central foil, i.e. the one labelled 5 in Figure 4.1, is centered on an axis defined by the deuteron beam directions. In ideal condition, this central indium is supposed to be centered on this axis. However, there is no way such can be assured. Hence, this lack of knowledge of the precise alignment of the indium foils introduces systematic error. To estimate this uncertainty, a quadratic surface was fitted to the experimental reaction rates calculated for each foil when there was a polyethylene plate covering the HFNG. The plot shows how much the central

indium foil was displaced from the origin, and the associated uncertainty. Using the uncertainty, the position of the indium foils in the MCNP simulation were adjusted and simulations carried out to determine the upper and lower limits of the systematic error. Table 4.11 and Table 4.12 show the systematic error while Figure *4.4* and Figure *4.5* show plots of the systematic error superimposed on the statistical error.

Foil	Simulation/experiment	Lower systematic error	Upper systematic error
1	0.86	0.03	0.02
2	1.20	0.01	0.04
3	1.12	0.09	0.12
4	0.72	0.04	0.02
5	1.06	0.01	0.02
6	1.22	0.002	0.06
7	0.90	0.06	0.06
8	1.01	0.03	0.03
9	1.25	0.08	0.03

Table 4.11. Simulation to experiment ratio for the first method, showing systematic error

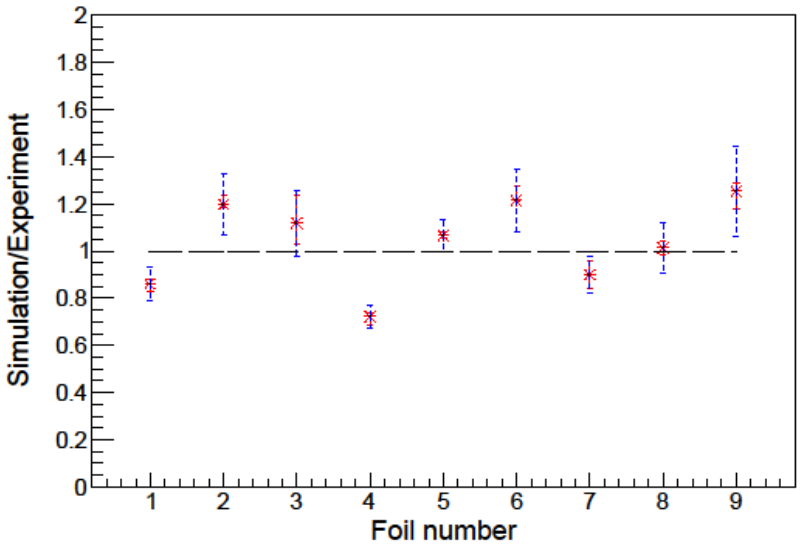

Figure 4.4. Comparison between experiment and simulation using the first method, with systematic error included. The solid red error bars are the systematic errors while the dashed blue error bars are the statistical errors.

Foil	Simulation/experiment	Lower limit of systematic error	Upper limit of systematic error
1	0.99	0.00	0.16
2	1.28	0.00	0.10
3	1.27	0.00	0.24
4	0.90	0.00	0.22
5	1.12	0.0	0.07
6	1.20	0.08	0.00
7	0.92	0.04	0.08
8	1.19	0.00	0.20
9	1.18	0.10	0.01

Table 4.12. The ratio of simulation to experiment for the second method, showing systematic error.

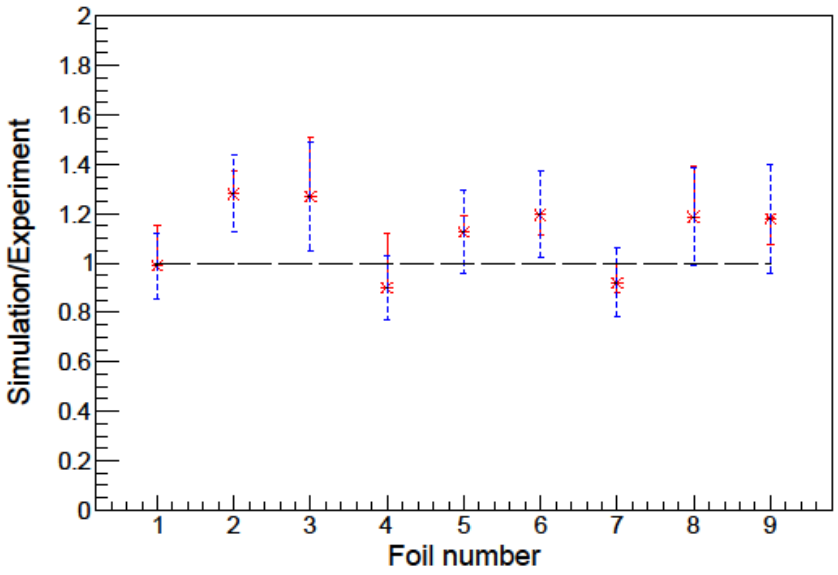

Figure 4.5. Comparison between experiment and simulation using the second method, with systematic error included. The solid red error bars are the systematic errors while the dashed blue error bars are the statistical errors.

5 Conclusions

Neutron generators such as D-D fusion generators can serve the purpose of performing integral benchmark experiment for validation of cross-section data. The Nuclear Engineering department of the University of California Berkeley has D-D neutron generator called the High Flux Neutron Generator (HFNG). It operates in the range of 100-125 keV of accelerating voltage.

Data on energy and angular distribution of neutrons produced in D-D fusion neutron generators at 100- and 150 keV are available on published literature. The data was interpolated to get the angular and energy distribution of neutrons at 105 keV. Using these interpolated data, an MCNP input file was constructed for two geometries: 1) with 20 cm thick polyethylene plates covering the HFNG. 2) with the polyethylene plates removed. A billion neutrons were simulated and ^{115m}In and ^{116m1}In production rates were computed.

For the experiment part, nine indium foil in a plastic holder with its plane at about I cm from the neutron production point, were irradiated first with the polyethylene plates in place and then without the polyethylene, for four hours each. The 336- and 416 keV gamma photon from inelastic scattering and radiative capture in indium were counted and used to compute single and double ratios. The double ratio makes use of the fact that ^{115m}In is only sensitive to the primary neutrons in the generator, and not scattered one. This makes its rate of production constant in both irradiations.

For the single ratio, the ratio of ^{116m1}In production in the presence of the polyethylene plate to that in the absence of polyethylene plates was compared between experiment and simulation. The result for each foils ware computed. The central indium foil showed excellent agreement with the expected value of unity. Most other foils only showed good agreement. The lack of excellent agreement with most other foils might be due to error in the angular dependence of neutron yield in $d(d,n)^3He$ reaction, particularly in performing interpolation. If this is accounted for, perhaps those foils might show excellent agreement with the expected value of unity.

For the double ratio method, an excellent agreement between experiment and simulation was also obtained for the central indium foil, showing that $^{115}In(n,n')^{115m}In$ reaction is not sensitive to neutrons scattered back by the polyethylene plates and other structures, notably the aluminum body. Like the single ratio, the value for other foils mostly shows good agreement between experiment and simulation.

From the foregoing, the scattering cross-section for carbon and hydrogen in ENDF/B-VII.1 agrees to experimental data within limit of experimental errors.

Deconvoluting the experimental data to separately compare scattering data for carbon and hydrogen between simulation and experiment might be a worthwhile research to pursue.

Bibliography

[1] J.-C. Sublet, “Nuclear Data Validation and Re-evaluation by Means of Integral Experiments,” *J. Nucl. Sci. Technol.*, vol. 37, pp. 708–712, 2000.

[2] I. C. Gauld, M. L. Williams, F. Michel-Sendis, and J. S. Martinez, “Integral nuclear data validation using experimental spent nuclear fuel compositions,” *Nucl. Eng. Technol.*, vol. 49, no. 6, pp. 1226–1233, Sep. 2017.

[3] G. Palmiotti, “Integral Experiments Analysis for Validation and Improvement of Minor Actinide Data for Transmutation Needs,” in *AIP Conference Proceedings*, 2005, vol. 769, pp. 1436–1441.

[4] C. Chabert, A. Santamarina, and P. Bioux, “Trends in Nuclear Data Derived from Integral Experiments in Thermal and Epithermal Reactors,” *J. Nucl. Sci. Technol.*, vol. 39, no. sup2, pp. 868–871, Aug. 2002.

[5] K. S. Krane, *Introductory Nuclear Physics*. Hoboken, NJ: Wiley & Sons, Inc, 1988.

[6] M. L. E. Oliphant, P. Harteck, and Lord Rutherford, “Transmutation Effects Observed with Heavy Hydrogen,” *Proc. R. Soc. A Math. Phys. Eng. Sci.*, vol. 144, no. 853, pp. 692–703, 1934.

[7] J. Schwinger, “On the Charge Independence of Nuclear Forces,” *Phys. Rev.*, vol. 78, no. 2, pp. 135–139, Apr. 1950.

[8] J. Csikai, *CRC Handbook of Fast Neutron Generators*. CRC.

[9] H. Liskien and A. Paulsen, “Neutron production cross sections and energies for the reactions T(p,n)3He, D(d,n)3He, and T(d,n)4He,” *Topics in Catalysis*, vol. 11, no. 7. Academic Press, pp. 569–619, 01-Jun-1973.

[10] J. F. Ziegler and J. P. Biersack, *SRIM, the Stopping and*

Range of Ions in Matter. Co, 2008.
[11] C. Waltz, “Characterization of Deuteron-Deuteron Neutron Generators,” 2016.
[12] C. J. Seagrave, J. D., Graves, E. R., Hipwood, S. J., and McDole, “D(d,) 3He and T(p,n)3He Neutron Source Handbook,” Los Alamos, 1958.
[13] “Interactive Chart of Nuclides.” [Online]. Available: http://www.nndc.bnl.gov/chart/. [Accessed: 21-Oct-2017].
[14] “No Title.” [Online]. Available: http://atom.kaeri.re.kr/nuchart/. [Accessed: 01-Oct-2017].
[15] R. Brun and F. Rademakers, “ROOT - An object oriented data analysis framework,” *Nucl. Instruments Methods Phys. Res. Sect. A Accel. Spectrometers, Detect. Assoc. Equip.*, vol. 389, no. 1–2, pp. 81–86, Apr. 1997.
[16] “Table of Isotopes decay data.” [Online]. Available: http://nucleardata.nuclear.lu.se/toi/nuclide.asp?iZA=490416. [Accessed: 19-Oct-2017].
[17] C. G. Ryan, E. Clayton, W. L. Griffin, S. H. Sie, and D. R. Cousens, “SNIP, a statistics-sensitive background treatment for the quantitative analysis of PIXE spectra in geoscience applications,” *Nucl. Instruments Methods Phys. Res. Sect. B Beam Interact. with Mater. Atoms*, vol. 34, no. 3, pp. 396–402, Sep. 1988.
[18] N. Otuka *et al.*, “Towards a More Complete and Accurate Experimental Nuclear Reaction Data Library (EXFOR): International Collaboration Between Nuclear Reaction Data Centres (NRDC),” *Nucl. Data Sheets*, vol. 120, pp. 272–276, Jun. 2014.
[19] “ENDF/B-VII.1 Nuclear Data for Science and Technology: Cross Sections, Covariances, Fission Product Yields and Decay Data,” *Nucl. Data Sheets*, vol. 112, no. 12, pp. 2887–

2996, Dec. 2011.
[20] “sigma.” [Online]. Available: https://www.nndc.bnl.gov/sigma/. [Accessed: 19-Oct-2017].
[21] A. T. R. Capote, K.L. Zolotarev, V.G. Pronyaev, “Updating and extending the IFDR-2002 Dosimetry Library - 2011,” in *proceedings of the International Symposium on Reactor Dosimetry (ISDR-14)*, 2011, p. 197.

Appendix A MCNP input file

A.1 Rate simulation in presence of Polyethylene plate covers.

Below is the input file for the calculated of the rate of production of the two metastable states of indium, ^{115m}In and ^{116m1}In when the HFNG chamber is surrounded with polyethylene plates.

```
Title - Etcheverry HFNG Room Shielding for BGC
C ------------------------------------------------------------------------------
C Cells
C ------------------------------------------------------------------------------
C 1  50  -7.31  -1 2 -3 4 -5 6                    IMP:N,P=1 $indium foil location.
1  50  -7.31  -1 -3 4                      IMP:N,P=1 $indium foil location.
9  100 -2.7  (-10 11 18 -20 21) : (-12 13 -18 19 -20 21 34)
          : (14 -15 -18 19 -20 21 34)
          : (-16 17 -19 -20 21) : (-22 23 20 18)
          : (-24 25 -19 20) : (-26 27 20 -18 19) $ 921
          : (-30 31 -21 18) : (-32 33 -21 -19)
          : (-28 29 -21 -18 19)                IMP:N,P=1 $ Al Shroud
10 100 -2.7 -101 103 -104 (102:-105:106) 107 -108 109 110:
     (102:-105:106) -101 (102:117) -107 111          IMP:n,p=1 $ Aluminum Chamber w/Rest
11 910 -2.65 (-820 821:822 -823) -109               IMP:n,p=1 $ Quartz Window Chamber
15 100 -2.7 -250 251 272 -252                    IMP:n,p=1 $ Elbow
16 100 -2.7 -256 (-222:-255) (102:221) 254 -302 252      IMP:n,p=1 $ Reducer
17 100 -2.624 -270 -272 271                      IMP:n,p=1 $ Turbo Pump
20 200 -0.955 (108 -101 103 -104 (-130:143 -144 (-141:145) (-142:-146)) -212)
     (-133:134:-135 131:136 132:210) #155 #22       IMP:n,p=1 $ Poly Shielding
C 20 200 -0.955 #21 205 -206 207 -208 111 -212 (-201:202:-203:204:213) 150:
C      (108 -101 103 -104 (-130:143 -144 (-141:145) (-142:-146)) -212)
C      (-133:134:-135 131:136 132:210) #155 #22         IMP:n,p=1 $ Poly Shielding
21 600 -1.23E-3  -942 202 -206                   IMP:n,p=1 $ Hole in poly
22 100 -2.7 -130 108 -101 103 -104 (131:132:-133:134) 921 #99  IMP:n,p=1 $ Al Top of
Chamber
24 200 -0.955 #21 205 -206 207 -208 111 -212
          (-201:202:-203:204:213) 150              IMP:n,p=1 $ Reflector
C 130 0 (-205:206:-207:208:211) (305 -306 307 -308 209 -311) IMP:n,p=1 $ Lead
30 100 -2.7 -303 302 -111 102:316 -317 -314 315        IMP:n,p=1 $ Aluminum Table
C 41 400 -8.92 411 -421 431 -441 92 -93              IMP:n,p=1 $ Target Magnets removed -
turned into copper
C 41 300 -7.4 411 -421 431 -441 92 -93               IMP:n,p=1 $ Target Magnets
C 42 LIKE 41 BUT TRCL=42
C 43 LIKE 41 BUT TRCL=43
C 44 LIKE 41 BUT TRCL=44
```

```
51 0 512 -513 514 -515 #1                    u=2     IMP:n,p=1
C  52 0  #51 #61                             u=2     IMP:n,p=1 $ Copper Segment made VOID
52 400 -8.92 #51 #61                         u=2     IMP:n,p=1 $ Copper Segment
C fill V groove and Water Channel with Copper
61 500 -1.0 -600:-599                        u=2     IMP:n,p=1 $ Water Channel
c 61 500 -1.0  (602:-601) 606:(601:-602) -605       u=2     IMP:n,p=1 $ Water Channel
c 71 400 -8.92 (700 -701:-705 706) 514 -515         u=2     IMP:n,p=1 $ V groove
c 61 500 -1 (602:-601) 606:(601:-602) -605          u=2     IMP:n,p=1 $ Water Channel
c 71 0 (700 -701:-705 706) 514 -515                 u=2     IMP:n,p=1 $ V groove
150 0 603 -604 504 -505 u=1 lat=1 fill=-6:6 0:0 0:0
     2 2 2 2 2 2 2 2 2 2 2 2 2 trcl=(-0.25399 0 0)        IMP:n,p=1 $ Target component fill
151 0 90 -91 502 -503 92 -93 fill=1                       IMP:n,p=1 $ Target
152 400 -8.92 ((502 -503 (500 -90:91 -501) 92 -93):
     ((-92 504:93 -505) 500 -501 502 -503))
                  #153 #154                  IMP:n,p=1  $ Target Wings      & Caps
153 0 516 -517 514 -515 (500 -90:-501 91)          IMP:n,p=1 $ Wing Slot
154 500 -1 420 -421 440 -441 (-92 94:93 -95)       IMP:n,p=1 $ Target Water Bath
155 100 -2.7 -921 -922 26  505                     IMP:n,p=1
C Cell 100-115 Source Magnets
100 300 -7.4 (120 -122 -124 125 -126 128):         $ Ion Source Magnets
           (-121 123 -124 125 -126 128)         IMP:n,p=1
101 LIKE 100 BUT TRCL=101
102 LIKE 100 BUT TRCL=102
103 LIKE 100 BUT TRCL=103
104 LIKE 100 BUT TRCL=104
105 LIKE 100 BUT TRCL=105
106 LIKE 100 BUT TRCL=106
107 LIKE 100 BUT TRCL=107
108 LIKE 100 BUT TRCL=108
109 LIKE 100 BUT TRCL=109
110 LIKE 100 BUT TRCL=110
111 LIKE 100 BUT TRCL=111
112 LIKE 100 BUT TRCL=112
113 LIKE 100 BUT TRCL=113
114 LIKE 100 BUT TRCL=114
115 LIKE 100 BUT TRCL=115
C Cell 80 Copper Sources
80 400 -8.92 ((800 -802 -110 804):
     (-801 803 -110 804)) #100 #101 #102 #103
     #104 #105 #106 #107 #108 #109
     #110 #111 #112 #113 #114 #115              IMP:n,p=1 $ Ion Source
120 501 1E-6 (800 -802 -804):(-801 803 -804)       IMP:n,p=1 $ Plasma
220   0 -118 (-105 520  : 106 -519 )               IMP:n,p=1 $ Vacuum
221 900 -10.28 ( 519 -800 35 : -520 801 35) -110   IMP:n,p=1 $ Extraction Plate
222 0 ( 519 -800 -35 : -520 801 -35)               IMP:n,p=1 $ Extraction Plate Hole
230 910 -2.65 (802 -812 : -803 813) -110           IMP:n,p=1 $ Quartz Plate
```

```
231 100 -2.7  (-105 520 : 106 -519) -110 118       IMP:n,p=1 $ Al Spacer
C Cell 90 Room Air
90 600 -1.23E-3 (201 -202 203 -204 107 -130 (101:-103:104) (110:812:-813):
    201 -202 203 -204 -107 101 111:
    -150 -212 130 (-143:144:-145 141:146 142):
    150 130 -213 201 -202 203 -204:
    ((-821 201:823 -202) -109):
    209 -909 -907 (932:-931:220) (-934:935) 905 901 -903
    (((-205:206:-207:208:212) 314:317 270:-271):
    -907 -315 209 250 272 (932:-931) 901 -903:
    271 -272 270 -315 209:
    205 -206 207 -208 (-111 (303:-302) (256:222) 255 252:
    315 (-316:314) 250 -252)):907 -908 -910 -940)
    #155                                IMP:n,p=1
91 600 -1.23E-3  -942 907 -946                    IMP:n,p=1  $ Side hole (3")
92 600 -1.23E-3  -945 946 -941                    IMP:n,p=1  $ Side hole (4.5")
93 600 -1.23E-3  -943 941 -908                    IMP:n,p=1  $ Side hole (6")
94 600 -1.23E-3  -944 907 -908                    IMP:n,p=1  $ Angled hole
95 600 -1.23E-3  -940 909 -910                    IMP:n,p=1  $ Top hole
C Concrete Walls
86 800 -2.4 -209 321 912 -914 916 -918 (-902:904:-906:908)  IMP:n,p=1
88 800 -2.4 (909 940:-901:903:-905:907:-209)
      902 -904 906 -908 -910 321
      (943:-941) (942:-907) (945:-946) (944:-907)         IMP:n,p=1
89 800 -2.4 209 -220 931 -907 -932 901                   IMP:n,p=1
87 800 -2.4 220 -909 901 -907 -935 934                   IMP:n,p=1
C Cell 99 - Vacuum Inside
99 0 ((-500:501:-502:503:-504:505) (105 -106:-117) (-221:-254) 252
    -108 (-102:-109 820 -822):-251 -252 272:
    108 133 -134 (135:-131) (-136:-132) -210 -212) #155 #9 IMP:n,p=1
C Beam Stop
1000 201 -0.955     -1000 1010 1020                  IMP:n,p=1
1010 600 -1.23E-3  -1010                          IMP:n,p=1
1020 600 -1.23E-3  -1020                          IMP:n,p=1
C Outside boundary
199 600 -1.23E-3  998 (910:908:904:-902:-906)
              209 -920 -918 -914 912 916 1000         IMP:n,p=1
998 600 -1.23E-3 -998                             IMP:n,p=1
C Non-important Zone outside
999 0 920:918:-916:914:-912:-321                     IMP:n,p=0

C ------------------------------------------------------------------------------
C Surfaces
C ------------------------------------------------------------------------------
C --------------------------- Shroud Surfaces ------------------------
C plates with cylindrical caps on top, bottom, and sides, quadrants of spheres cap corners
```

```
C -------------------------------------------------------------------------------
C 1   PX   2.5
1   CY   0.43 $0.495
2   PX  -2.5
3   PY   0.025
4   PY  -0.025
5   PZ   2.5
6   PZ   -2.5
10  C/Z  6.7916 0. 3.2385
11  C/Z  6.7916 0. 2.9795
12  PY   3.2385
13  PY   2.9795
14  PY  -3.2385
15  PY  -2.9795
16  C/Z -6.7916 0. 3.2385
17  C/Z -6.7916 0. 2.9795
18  PX   6.7916
19  PX  -6.7916
20  PZ   6.7916
21  PZ  -6.7916
22  S    6.7916 0. 6.7916 3.2385
23  S    6.7916 0. 6.7916 2.9795
24  S   -6.7916 0. 6.7916 3.2385
25  S   -6.7916 0. 6.7916 2.9795
26  C/X  0. 6.7916 3.2385
27  C/X  0. 6.7916 2.9795
28  C/X  0. -6.7916 3.2385
29  C/X  0. -6.7916 2.9795
30  S    6.7916 0. -6.7916 3.2385
31  S    6.7916 0. -6.7916 2.9795
32  S   -6.7916 0. -6.7916 3.2385
33  S   -6.7916 0. -6.7916 2.9795
34  CY   2.032
35  CY   0.15875  $ hole in extraction plate
C  -------------------------------Vacuum Vessel Surfaces--------------------------
101 CZ  18.503                $ Outer cylindrical surface
102 CZ  15.9                  $ Inner cylindrical surface
103 PY  -9.627                $ Outer planar surface 1
104 PY   9.627                $ Outer planar surface 2  10.281cm
105 PY  -7.087                $ Inner planar surface 1
106 PY   7.087                $ Inner planar surface 2
107 PZ  -14                   $ Bottom Bound
108 PZ   14                   $ Top Bound
109 CX   3.4925                $ Gauge/Equipment Holes
110 CY   9.5                  $ Ion Source Holes
111 PZ  -24                   $ Chamber Rest Bottom Bound
```

```
117 PZ  -16                  $ Bottom Chamber Lip bottom
118 CY   4.255                 $ Al Spacer
519 PY  10.281                 $ Extraction Plate
520 PY -10.281                 $ Extraction Plate
130 PZ   16.5                $ HV Insulator
131 C/Z -3.5 0 2
132 C/Z  3.5 0 2
133 PY  -2
134 PY   2
135 PX  -3.5
136 PX   3.5
141 C/Z -3.5 0 4.5
142 C/Z  3.5 0 4.5
143 PY  -4.5
144 PY   4.5
145 PX  -4.5
146 PX   4.5
150 CZ  10
201 PX -20
202 PX 20          $ Shielding Surfaces
203 PY -20
204 PY 20
205 PX -40.32
206 PX 40.32
207 PY -40.32
C For PY and PXs below and above, the oriinal is 40.32 cm. But I extended it to accommodate
the reflector
C It should be brought back at the end of reflector study.
208 PY 40.32
209 PZ -229        $ Floor
210 PZ 44.5
211 PZ 70
212 PZ 47    $original is 47
213 PZ 27
220 PZ -169
221 KZ -64.225 0.2158 1
222 KZ -65 0.2158 1
250 TY -30 0 -46 30 10.3 10.3  $ Elbow
251 TY -30 0 -46 30 10   10
252 PZ -46     $ original -46
253 PZ -42.7
254 CZ 10
255 CZ 10.3
256 CZ 16.2
270 C/X 0 -76 12.1       $ Turbo Pump
271 PX -59  $original -59
```

```
272 PX -30
C Table Surfaces
302 PZ -26.54          $ Bottom of Top Aluminum Frame Shelf
303 CZ 33      $ emeka. 33 is original
314 PZ -55.75
315 PZ -57             $ Bottom of Bottom Al Frame Shelf
316 CZ 28.3           $ original is 28.3
317 CZ 58.2   $ emeka. Original is 58.2 cm
C Lead Outer Surfaces
305 PX -75
306 PX 75
307 PY -75
308 PY 75
311 PZ 75
321 PZ -329      $ Concrete Floor Bottom
325 PX -100
326 PX 100
327 PY -100
328 PY 100
C Concrete Walls
901 PY -233
902 PY -381
903 PY  231
904 PY  479
905 10 PX -232
906 10 PX -288
907 10 PX  232  $original size is 232
908 10 PX  387
909 PZ 197
910 PZ 456
931 10 PX  22
932 PY -60 $ original is 60
934 10 PX 125
935 PY -126
940 C/Z 11 -36 7.62        $ Roof Penetration
941 10 PX 335
942 C/X 0 0 3.81        $ 3" to 6" penetration
943 C/X 0 0 7.62
944 900 CX 7.62            $ Angled Penetration
945 C/X 0 0 5.715
946 10 PX 283
C Outside boundary
912 PY -401
914 PY 499
916 10 PX -308
918 10 PX 707
```

```
920 PZ 476
921 CZ 0.95
922 PZ 100
C ------------------------- Beam Stop -------------------------------------
1000 10 RPP 482 562  -30 30  -30 30
1010 10 RCC 482 0 0  25 0 0  10
1020 10 RCC 507 0 0  25 0 0  20
C ------------------------ Target Surfaces --------------------------------
C Target Magnets
411 PX  3.3225
420 PX -3.9575
421 PX  3.9575
431 PY  0.2285
440 PY -0.8440 $-0.8635
441 PY  0.8440 $0.8635
C Target Box
500 PX -4.445
501 PX  4.445
502 PY -0.9525 $-0.8448  $-1.031
503 PY  0.9525 $ 0.8448  $ 1.031
504 PZ -4.66 $-5.08
505 PZ  4.66 $5.08
C Sample Box
512 PY -0.2667 $-0.159
513 PY  0.2667 $0.159
514 PZ -3.175
515 PZ  3.175
516 PY -0.159
517 PY  0.159
C Water Channels
599 C/Z 0. -0.5207 0.1778 $ -0.457 old-y
600 C/Z 0.  0.5207 0.1778 $  0.457
C 601 P 1 0.414 0 0
C 602 P 1 -0.414 0 0
603 PX  -0.254  $-0.357
604 PX   0.254  $ 0.357
605 PY -0.25
606 PY  0.25
C V-grooves
c 700 P 1 0.414 0 0.09
c 701 P 1 -0.414 0 -0.09
C 700 PX  0.357
C 701 PX -0.357
C 702 PZ -3.105
C  703 PZ 3.105
c 705 P 1 0.414 0 -0.09
```

```
c 706 P 1 -0.414 0 0.09
C   705 PX -0.357
C   706 PX  0.357
90 PX  -2.54 $-2.286 $ -3.213 $ Non-universe target surfaces
91 PX   2.54 $ 3.213
92 PZ -3.81
93 PZ  3.81
94 PZ -4.29
95 PZ  4.29
C Ion Sources Surfaces
800 PY  10.598 $9.9445 $9.3095  $7.4
801 PY -10.598 $-9.9445 $-9.3095 $-7.4
802 PY 16.313 $15.8575  $15.54   $13.3
803 PY -16.313 $-15.8575 $-15.54  $-13.3
804 CY 6.19
812 PY 16.948  $ 16.64 $14.1
813 PY -16.948 $-16.64 $-14.1
C Ion Source Magnet
120 PY  10.8907 $10.575  $8.035      $ Ion Source Magnets
121 PY -10.9907 $-10.575 $-8.035
122 PY  14.7025  $14.385  $11.845
123 PY -14.7025 $-14.385 $-11.845
124 PX 0.635
125 PX -0.635
126 PZ 8.447
127 PZ -8.447
128 PZ 7.177
129 PZ -7.177
C ---------------------
820 PX -17.36          $ Quartz Window Chamber
821 PX -18
822 PX 17.36
823 PX 18
C ---------------------
998 RCC 227.0001 0 0 .0001 0 0 3.81
C Reflector
11901 PX 20
11902 PX -20
11903 PY 37
11904 PY 22
11905 PZ -13
11906 PZ 13

C ------------------------------------------------------------------------
C Data
C ------------------------------------------------------------------------
```

```
TR10 -170 0 0   $ Room transformation to accomodate generator
C Magnet Coordinate Transformations
TR4   0     -0.05    0
TR42  -7.28   0      0
TR43  0      -1.092  0
TR44  -7.28  -1.092  0
TR62  -0.714  0      0
TR63  -1.428  0      0
TR64  -2.142  0      0
TR65   0.714  0      0
TR66   1.428  0      0
TR67   2.142  0      0
TR68   2.856  0      0
TR72  -0.714  0      0
TR73  -1.428 0 0
TR74  -2.142 0 0
TR75  -2.856 0 0
TR76   0.714 0 0
TR77   1.428 0 0
TR78   2.142 0 0
TR79   2.856 0 0
TR101  0 0 0 0.9239 0 -0.3827 0 1 0 0.3827 0 0.9239
TR102  0 0 0 0.7071 0 -0.7071 0 1 0 0.7071 0 0.7071
TR103  0 0 0 0.3827 0 -0.9239 0 1 0 0.9239 0 0.3827
TR104  0 0 0 0 0 -1 0 1 0 1 0 1
TR105  0 0 0 -0.3827 0 -0.9239 0 1 0 0.9239 0 -0.3827
TR106  0 0 0 -0.7071 0 -0.7071 0 1 0 0.7071 0 -0.7071
TR107  0 0 0 -0.9239 0 -0.3827 0 1 0 0.3827 0 -0.9239
TR108  0 0 0 -1 0 0 0 1 0 0 0 -1
TR109  0 0 0 -0.9239 0 0.3827 0 1 0 -0.3827 0 -0.9239
TR110  0 0 0 -0.7071 0 0.7071 0 1 0 -0.7071 0 -0.7071
TR111  0 0 0 -0.3827 0 0.9239 0 1 0 -0.9239 0 -0.3827
TR112  0 0 0 0 0 1 0 1 0 -1 0 0
TR113  0 0 0 0.3827 0 0.9239 0 1 0 -0.9239 0 0.3827
TR114  0 0 0 0.7071 0 0.7071 0 1 0 -0.7071 0 0.7071
TR115  0 0 0 0.9239 0 0.3827 0 1 0 -0.3827 0 0.9239
TR900  62 -41 51 0.707 0.707 0 -0.707 0.707 0 0 0 1
C ------------------------------------------------------------------------
C Materials for Geometry-----------------------------------------------------
C ------------------------------------------------------------------------
M50 49113 0.0429 49115 0.9571     $ Natural Indium
M60 49115   1.0     $ In-115
M100   13027 1 $ Aluminum
M200   6000  0.3333 $ Polyethylene
      1001  0.6667
M201   6000  37.5  $ Polyethylene + Boron 5 percent weight
```

```
      1001  74.985
      1002  0.015
      5010  0.588 $ B-10
      5011  2.412 $ B-11
M300   60142 0.032 $ Nd-Fe-B Magnets
      60143 0.014
      60144 0.028
      60145 0.010
      60146 0.020
      60148 0.007
      60150 0.007
      26054 0.047792
      26056 0.755773
      26057 0.018128
      26058 0.002307
      5010  0.0116
      5011  0.0464
M301 26054 1
M302 26058 1
M303 60142 1
M304 60143 1
M305 60144 1
M306 60146 1
M400  29063 0.6915 $ Copper-63
     29065 0.3085 $ Copper-65
M401  29063 1
M402  29065 1
M500  1001 0.667 $ Water
     8016 0.333
M501  1002 1
M600  8016       -0.232       $ Dry Air
     7014       -0.754
     18040      -0.014
C M700  82000 1 $ Lead
M800  1001  -0.0221   $ Concrete
     6000  -0.002484
     8016  -0.574930
     11023 -0.015208
     12024 -0.001000013
     12025 -0.0001266
     12026 -0.000139387
     13027 -0.019953
     14028  -0.280936158
     14029  -0.014271775
     14030  -0.009419067
     19039 -0.009367776
```

```
     19041 -0.000677224
           20040 -0.041719165
           20042 -0.000277893
     20043 -0.000057984
     20044       -0.000895958
     26054   -0.000376126
     26056   -0.00590437
     26057   -0.000136358
     26058         -0.000018147
M900  42092  0.1484    $ Moly plate
     42094  0.0925
     42095  0.1592
     42096  0.1668
     42097  0.0955
     42098  0.2413
     42100  0.0963
M901  42098  1
M910  14028 0.3074      $ Quartz
     14029 0.0156
     14030 0.0103
     8016 0.6667
M911  14030 1
C **********REFLECTOR MATERIALS**********
 M9112 6012 1. $Carbon
 M9113 20040 1. $Ca-40
 M9114 82208 1. $Pb-208
 M9115 20040 0.1939   $ Calcium Carbonate.
     20040 0.001294
     20040 0.00027
     20040 0.004172
     6012  0.1979
     6013  0.00214
     8016  0.5985
     8016  0.00023
     8016  0.00123
M9116 26056 1. $Iron
M9117 6000 1. $natural Carbon
M9118 26054   0.05845  $natural Iron
     26056   0.91754
     26057   0.02119
     26058         0.00282
M9119 82204   0.014  $natural Pb
           82206   0.241
     82207   0.221
     82208   0.524
M9120 5010 1. $Boron
```

```
C Scattering Kernels
C MT100 al27 $ Aluminum
C MT200 poly $ natural polyethylene
C MT201 poly $ borated polyethylene
C MT300 fe56 $ Iron
C MT500 lwtr $ Hydrogen in Light Water
C ------------------------------------------------------------------------
C ---- Mesh Tallies ----- When using 2 sources the factor below should be doubled
C ------------------------------------------------------------------------
C FMESH14:N origin=0 -401 -2.5 imesh=540 jmesh=499 kmesh=2.5
C         iints=108 jints=180 kints=1 factor=1.08e08
C DE14   1.0E-9 1.0E-8 2.5E-8 1.0E-7 2.0E-7 5.0E-7 1.0E-6 2.0E-6 5.0E-6
C      1.0E-5 2.0E-5 5.0E-5 1.0E-4 2.0E-4 5.0E-4 1.0E-3 2.0E-3 5.0E-3
C      0.0100 0.0200 0.0300 0.0500 0.0700 0.1000 0.1500 0.2000 0.3000
C      0.5000 0.7000 0.9000 1.0000 1.2000 1.5000 2.0000 3.0000
C DF14   1.7    2.03   2.31   2.98   3.36   3.86   4.17   4.40   4.59
C      4.68   4.72   4.73   4.72   4.67   4.60   4.58   4.61   4.86
C      5.57   7.41   9.46   13.7   18.0   24.3   34.7   44.7   63.8
C      99.1   131    160    174    193    219    254    301
C FMESH24:P origin=0 -401 -2.5 imesh=540 jmesh=499 kmesh=2.5
C         iints=108 jints=180 kints=1 factor=1.08e08
C DE24   0.010 0.015 0.020 0.030 0.040 0.050 0.060 0.070 0.080 0.100 0.150
C      0.200 0.300 0.400 0.500 0.511 0.600 0.662 0.800 1.000 1.117 1.333
C      1.500 2.000 3.000 4.000 5.000 6.000 6.129 8.000 10.00 15.00 20.00
C DF24   .0337 .0664 .0986 0.158 0.199 0.226 0.248 0.273 0.297 0.355 0.528
C      0.721 1.120 1.520 1.920 1.960 2.300 2.540 3.040 3.720 4.100 4.750
C      5.240 6.550 8.840 10.80 12.70 14.40 14.60 17.60 20.60 27.70 34.40
C FMESH34:N origin=-40 -40 -40 imesh=40 jmesh=40 kmesh=40
C      iints=40 jints=40 kints=40 factor=1.0e08
C DE34   0.010 0.015 0.020 0.030 0.040 0.050 0.060 0.070 0.080 0.100 0.150
C      0.200 0.300 0.400 0.500 0.511 0.600 0.662 0.800 1.000 1.117 1.333
C      1.500 2.000 3.000 4.000 5.000 6.000 6.129 8.000 10.00 15.00 20.00
C DF34   .0337 .0664 .0986 0.158 0.199 0.226 0.248 0.273 0.297 0.355 0.528
C      0.721 1.120 1.520 1.920 1.960 2.300 2.540 3.040 3.720 4.100 4.750
C      5.240 6.550 8.840 10.80 12.70 14.40 14.60 17.60 20.60 27.70 34.40
C FMESH44:N origin=-40 -40 -40 imesh=40 jmesh=40 kmesh=40
C      iints=40 jints=40 kints=40 factor=1.0e08
C FMESH64:N geom=cyl origin = 217. 0. 0. axs=0 1 0 vec=0 0 1
C               imesh=7.62 jmesh=0.25 kmesh=1
C               iints=1 jints=1 kints=1
C FMESH74:N geom=cyl origin = 0.0 1.62 0.0 axs=0 1 0 vec=0 0 1
C               imesh=1 jmesh=0.0001 kmesh=1
C               iints=1 jints=1 kints=1 emesh=3. eints=200
C FMESH104:N geom=cyl origin= 0. -0.065 0. axs=0 1 0 vec=1 0 0
C               imesh=0.425 jmesh=0.025 kmesh=1
C               iints=1 jints=1 kints=1 emesh=3. eints=1200
```

```
C FMESH114:N geom=cyl origin= 1.0 -0.065 0. axs=0 1 0 vec=1 0 0
C                imesh=0.425 jmesh=0.025 kmesh=1
C                iints=1 jints=1 kints=1 emesh=3. eints=1200
C FMESH144:N geom=cyl origin= 1. -0.065 1. axs=0 1 0 vec=1 0 0
C               imesh=0.425 jmesh=0.025 kmesh=1
C                iints=1 jints=1 kints=1 emesh=3. eints=1200
C FMESH154:N geom=cyl origin= 0. 16.95 0. axs=0 1 0 vec=1 0 0
C                imesh=1.0 jmesh=0.025 kmesh=1
C                iints=1 jints=1 kints=1 emesh=3. eints=1200
C     #####
E0 0 200i 3
C F11:n (1 2 3 4 5 6)
C C11 0 1
C F21:n 4
F12:n 4
SD12 0.7699
FM12 0.03827 50 51
F102:n 4
SD102 0.7699
FM102 0.03827 50 102
FMESH64:N geom=cyl origin = 0.189 0 0.11 axs = 0 1 0 vec = 1 0 0
               imesh=0.495 jmesh=0.05 kmesh=1
               iints=1 jints=1 kints=1 emesh=0.4 2.8
                                   eints= 1 240
               factor 0.03848 $ volume of the fmesh
FM64 0.03827
FMESH4:N geom=cyl origin = 0.189 0 0.11 axs = 0 1 0 vec = 1 0 0
               imesh=0.495 jmesh=0.05 kmesh=1
               iints=1 jints=1 kints=1 emesh=3. eints=200
                                   factor=0.03848 $ volume of the fmesh
 FM4 0.03827 50 102
C
C Source - 0.25 cm radius disk sources located
C          outside the copper target holder
C
C SDEF POS=-0.05 -0.37 -0.686  &
C SDEF POS=0. 0. -0.686  &
C     AXS=0 0 1 VEC=0 0 1 RAD=D3 PAR=N DIR=D4 ERG=fdir D5 &
C     WGT=1.0 EXT=0
SDEF POS = 0.0 -1 0.0 &
     AXS=0 0 1 VEC=0 1 0 RAD=D3 PAR=1 DIR=D4 ERG=fdir D5 &
     WGT=1.0  EXT=0
C SI1 L  0 -1.1 0.  0 1.1 0.
C SP1 0.5  0.5
C  Distribution for axs
C SIn L 0 1 0 0 -1 0
```

```
C SPn 0.5 0.5
C  Distribution for vec
C  DS2 L 0 0 1
C  Distribution for rad
SI3   0 0.25
SP3 -21 1.0
C   Distribution for dir
C   This is cos(theta) in one-degree increments from 180 to 0 degreesou
C
SI4   -1    -0.99985    -0.99939    -0.99863    -0.99756 &
-0.99619    -0.99452    -0.99255    -0.99027    -0.98769 &
-0.98481    -0.98163    -0.97815    -0.97437     -0.9703 &
-0.96593    -0.96126     -0.9563    -0.95106    -0.94552 &
-0.93969    -0.93358    -0.92718     -0.9205    -0.91355 &
-0.90631    -0.89879    -0.89101    -0.88295    -0.87462 &
-0.86603    -0.85717    -0.84805    -0.83867    -0.82904 &
-0.81915    -0.80902    -0.79864    -0.78801    -0.77715 &
-0.76604    -0.75471    -0.74314    -0.73135    -0.71934 &
-0.70711    -0.69466      -0.682    -0.66913    -0.65606 &
-0.64279    -0.62932    -0.61566    -0.60182    -0.58779 &
-0.57358    -0.55919    -0.54464    -0.52992    -0.51504 &
-0.5        -0.48481    -0.46947    -0.45399    -0.43837 &
-0.42262    -0.40674    -0.39073    -0.37461    -0.35837 &
-0.34202    -0.32557    -0.30902    -0.29237    -0.27564 &
-0.25882    -0.24192    -0.22495    -0.20791    -0.19081 &
-0.17365    -0.15643    -0.13917    -0.12187    -0.10453 &
-0.087156   -0.069756   -0.052336   -0.034899   -0.017452 &
6.1232e-17   0.017452    0.034899    0.052336    0.069756 &
0.087156     0.10453     0.12187     0.13917     0.15643 &
0.17365     0.19081     0.20791     0.22495     0.24192 &
0.25882     0.27564     0.29237     0.30902     0.32557 &
0.34202     0.35837     0.37461     0.39073     0.40674 &
0.42262     0.43837     0.45399     0.46947     0.48481 &
0.5         0.51504     0.52992     0.54464     0.55919 &
0.57358     0.58779     0.60182     0.61566     0.62932 &
0.64279     0.65606     0.66913       0.682     0.69466 &
0.70711     0.71934     0.73135     0.74314     0.75471 &
0.76604     0.77715     0.78801     0.79864     0.80902 &
0.81915     0.82904     0.83867     0.84805     0.85717 &
0.86603     0.87462     0.88295     0.89101     0.89879 &
0.90631     0.91355      0.9205     0.92718     0.93358 &
0.93969     0.94552     0.95106      0.9563     0.96126 &
0.96593      0.9703     0.97437     0.97815     0.98163 &
0.98481     0.98769     0.99027     0.99255     0.99452 &
0.99619     0.99756     0.99863     0.99939     0.99985 &
1.0
```

```
C
C   ---------------------------------------------------------------------------
C   This is the secondary neutron angular distribution for incident deuterons of initial
C   energy of 100keV - uses Cory's reaction # to weight slowing down spectrum
C   (dsigma/domega)(theta)*domega normalized
C     From Liskiien -Paulsen
C   Error in previous computation - now corrected here
C   ---------------------------------------------------------------------------
SP4 0.000000000  0.000094925  0.000284665  0.000474124  0.000663135  &
0.000851536  0.001039164  0.001225856  0.001411450  0.001595787  &
0.001778707  0.001960052  0.002139668  0.002317400  0.002493096  &
0.002666609  0.002837791  0.003006499  0.003172594  0.003335940  &
0.003496403  0.003653857  0.003808177  0.003959246  0.004106950  &
0.004251182  0.004391841  0.004528831  0.004662064  0.004791458  &
0.004916940  0.005038441  0.005155905  0.005269279  0.005378522  &
0.005483600  0.005584487  0.005681169  0.005773637  0.005861895  &
0.005945953  0.006025832  0.006101562  0.006173183  0.006240742  &
0.006304297  0.006363913  0.006419665  0.006471636  0.006519917  &
0.006564607  0.006605812  0.006643644  0.006678224  0.006709676  &
0.006738133  0.006763730  0.006786608  0.006806913  0.006824792  &
0.006840396  0.006853879  0.006865397  0.006875103  0.006883157  &
0.006889712  0.006894925  0.006898950  0.006901939  0.006904042  &
0.006905404  0.006906170  0.006906477  0.006906460  0.006906249  &
0.006905968  0.006905734  0.006905659  0.006905850  0.006906404  &
0.006907414  0.006908964  0.006911131  0.006913985  0.006917587  &
0.006921990  0.006927242  0.006933379  0.006940432  0.006948423  &
0.006957366  0.006967266  0.006978123  0.006989926  0.007002659  &
0.007016296  0.007030806  0.007046149  0.007062279  0.007079141  &
0.007096675  0.007114813  0.007133483  0.007152602  0.007172086  &
0.007191841  0.007211768  0.007231762  0.007251715  0.007271510  &
0.007291025  0.007310136  0.007328710  0.007346613  0.007363703  &
0.007379835  0.007394861  0.007408626  0.007420975  0.007431745  &
0.007440774  0.007447895  0.007452937  0.007455728  0.007456095  &
0.007453861  0.007448849  0.007440880  0.007429777  0.007415359  &
0.007397449  0.007375870  0.007350445  0.007321001  0.007287368  &
0.007249376  0.007206863  0.007159670  0.007107642  0.007050632  &
0.006988499  0.006921108  0.006848335  0.006770061  0.006686181  &
0.006596595  0.006501218  0.006399974  0.006292801  0.006179649  &
0.006060480  0.005935271  0.005804014  0.005666714  0.005523393  &
0.005374087  0.005218848  0.005057745  0.004890862  0.004718300  &
0.004540175  0.004356622  0.004167788  0.003973840  0.003774957  &
0.003571336  0.003363187  0.003150736  0.002934220  0.002713892  &
0.002490016  0.002262869  0.002032735  0.001799913  0.001564708  &
0.001327433  0.001088409  0.000847961  0.000606422  0.000364126  &
0.000121410
C   -------------------------------------------
```

```
C      Neutron energy vs angle wtd as above
C     -----------------------------------------
DS5 2.1751  2.1752  2.1753  2.1755  2.1758  &
2.1762  2.1767  2.1773  2.1779  2.1787  &
2.1795  2.1804  2.1814  2.1825  2.1837  &
2.1849  2.1863  2.1877  2.1892  2.1908  &
2.1925  2.1942  2.1961  2.1980  2.2000  &
2.2021  2.2042  2.2065  2.2088  2.2112  &
2.2137  2.2162  2.2188  2.2215  2.2243  &
2.2271  2.2301  2.2330  2.2361  2.2392  &
2.2424  2.2457  2.2490  2.2524  2.2559  &
2.2594  2.2630  2.2666  2.2703  2.2741  &
2.2779  2.2818  2.2858  2.2898  2.2938  &
2.2979  2.3021  2.3063  2.3106  2.3149  &
2.3192  2.3237  2.3281  2.3326  2.3372  &
2.3418  2.3464  2.3511  2.3558  2.3605  &
2.3653  2.3702  2.3750  2.3799  2.3849  &
2.3898  2.3948  2.3999  2.4049  2.4100  &
2.4151  2.4202  2.4254  2.4306  2.4358  &
2.4410  2.4462  2.4515  2.4568  2.4621  &
2.4674  2.4727  2.4780  2.4833  2.4887  &
2.4940  2.4994  2.5047  2.5101  2.5154  &
2.5208  2.5261  2.5315  2.5368  2.5421  &
2.5475  2.5528  2.5581  2.5634  2.5686  &
2.5739  2.5791  2.5843  2.5895  2.5947  &
2.5998  2.6050  2.6101  2.6151  2.6201  &
2.6251  2.6301  2.6350  2.6399  2.6447  &
2.6495  2.6542  2.6589  2.6636  2.6682  &
2.6727  2.6772  2.6817  2.6860  2.6904  &
2.6946  2.6988  2.7030  2.7070  2.7110  &
2.7149  2.7188  2.7226  2.7263  2.7299  &
2.7335  2.7369  2.7403  2.7436  2.7469  &
2.7500  2.7530  2.7560  2.7589  2.7616  &
2.7643  2.7669  2.7694  2.7718  2.7741  &
2.7763  2.7784  2.7804  2.7823  2.7841  &
2.7858  2.7874  2.7888  2.7902  2.7915  &
2.7926  2.7937  2.7946  2.7955  2.7962  &
2.7968  2.7973  2.7977  2.7980  2.7981  &
2.7982
C  SP3    0. 0.01  0.99
C  SI3 -1 .992532 1   $ 7-degree cone towards hole, biased by 20x
C  SP3 0 0.996266 .003734
C  SB3 0 .05 .95
C FMESH tallys
FMESH2224:N geom=cyl origin = 0.189 0 1.11 axs = 0 1 0 vec = 1 0 0
            imesh=0.495 jmesh=0.05 kmesh=1
```

```
        iints=1 jints=1 kints=1 emesh=0.4 2.8
                                eints= 1 240
                                factor 0.03848 $ volume of the fmesh
FM2224 0.03827
FMESH2234:N geom=cyl origin = 0.189 0 1.11 axs = 0 1 0 vec = 1 0 0
        imesh=0.495 jmesh=0.05 kmesh=1
        iints=1 jints=1 kints=1 emesh=3. eints=200
                                factor=0.03848 $ volume of the fmesh
 FM2234 0.03827 50 102
FMESH2244:N geom=cyl origin = 1.189 0 0.11 axs = 0 1 0 vec = 1 0 0
        imesh=0.495 jmesh=0.05 kmesh=1
        iints=1 jints=1 kints=1 emesh=0.4 2.8
                                eints= 1 240
                                factor 0.03848 $ volume of the fmesh
FM2244 0.03827
FMESH2254:N geom=cyl origin = 1.189 0 0.11 axs = 0 1 0 vec = 1 0 0
        imesh=0.495 jmesh=0.05 kmesh=1
        iints=1 jints=1 kints=1 emesh=3. eints=200
                                factor=0.03848 $ volume of the fmesh
 FM2254 0.03827 50 102
FMESH2264:N geom=cyl origin = 1.189 0 1.11 axs = 0 1 0 vec = 1 0 0
        imesh=0.495 jmesh=0.05 kmesh=1
        iints=1 jints=1 kints=1 emesh=0.4 2.8
                                eints= 1 240
                                factor 0.03848 $ volume of the fmesh
FM2264 0.03827
FMESH2274:N geom=cyl origin = 1.189 0 1.11 axs = 0 1 0 vec = 1 0 0
        imesh=0.495 jmesh=0.05 kmesh=1
        iints=1 jints=1 kints=1 emesh=3. eints=200
                                factor=0.03848 $ volume of the fmesh
 FM2274 0.03827 50 102
FMESH2284:N geom=cyl origin = -0.811 0 0.11 axs = 0 1 0 vec = 1 0 0
        imesh=0.495 jmesh=0.05 kmesh=1
        iints=1 jints=1 kints=1 emesh=0.4 2.8
                                eints= 1 240
                                factor 0.03848 $ volume of the fmesh
FM2284 0.03827
FMESH2294:N geom=cyl origin = -0.811 0 0.11 axs = 0 1 0 vec = 1 0 0
        imesh=0.495 jmesh=0.05 kmesh=1
        iints=1 jints=1 kints=1 emesh=3. eints=200
                                factor=0.03848 $ volume of the fmesh
 FM2294 0.03827 50 102
FMESH3324:N geom=cyl origin = 0.189 0 -0.89 axs = 0 1 0 vec = 1 0 0
        imesh=0.495 jmesh=0.05 kmesh=1
        iints=1 jints=1 kints=1 emesh=0.4 2.8
                                eints= 1 240
```

```
                                factor 0.03848 $ volume of the fmesh
FM3324 0.03827
FMESH3334:N geom=cyl origin = 0.189 0 -0.89 axs = 0 1 0 vec = 1 0 0
          imesh=0.495 jmesh=0.05 kmesh=1
          iints=1 jints=1 kints=1 emesh=3. eints=200
                                factor=0.03848 $ volume of the fmesh
 FM3334 0.03827 50 102
FMESH3354:N geom=cyl origin = -0.811 0 -0.89 axs = 0 1 0 vec = 1 0 0
          imesh=0.495 jmesh=0.05 kmesh=1
          iints=1 jints=1 kints=1 emesh=0.4 2.8
                                eints= 1 240
                                factor 0.03848 $ volume of the fmesh
FM3354 0.03827
FMESH3364:N geom=cyl origin = -0.811 0 -0.89 axs = 0 1 0 vec = 1 0 0
          imesh=0.495 jmesh=0.05 kmesh=1
          iints=1 jints=1 kints=1 emesh=3. eints=200
                                factor=0.03848 $ volume of the fmesh
 FM3364 0.03827 50 102
FMESH3374:N geom=cyl origin = -0.811 0 1.11 axs = 0 1 0 vec = 1 0 0
          imesh=0.495 jmesh=0.05 kmesh=1
          iints=1 jints=1 kints=1 emesh=0.4 2.8
                                eints= 1 240
                                factor 0.03848 $ volume of the fmesh
FM3374 0.03827
FMESH3384:N geom=cyl origin = -0.811 0 1.11 axs = 0 1 0 vec = 1 0 0
          imesh=0.495 jmesh=0.05 kmesh=1
          iints=1 jints=1 kints=1 emesh=3. eints=200
                                factor=0.03848 $ volume of the fmesh
 FM3384 0.03827 50 102
FMESH3394:N geom=cyl origin = 1.189 0 -0.89 axs = 0 1 0 vec = 1 0 0
          imesh=0.495 jmesh=0.05 kmesh=1
          iints=1 jints=1 kints=1 emesh=0.4 2.8
                                eints= 1 240
                                factor 0.03848 $ volume of the fmesh
FM3394 0.03827
FMESH4404:N geom=cyl origin = 1.189 0 -0.89 axs = 0 1 0 vec = 1 0 0
          imesh=0.495 jmesh=0.05 kmesh=1
          iints=1 jints=1 kints=1 emesh=3. eints=200
                                factor=0.03848 $ volume of the fmesh
FM4404 0.03827 50 102
C FCL:n 1 1 0 34i 0
RAND GEN=2 STRIDE=152917 SEED=10899028731
NPS  1e9
C CUT:n j 1.5e-8
MODE n
C PTRAC  file=asc write=all event=src
```

```
C VOID 24
PRINT 110
C PRDMP 2J 1
```

C.2 **Rate simulation in the absence of Polyethylene plate covers**.

The input file calculated the rate of production of the two metastable states of indium, ^{115m}In and ^{116m1}In when there are no polyethylene plates present.

```
Title - Etcheverry HFNG Room Shielding for BGC
C ------------------------------------------------------------------------------
C Cells
C ------------------------------------------------------------------------------
1  50  -7.31  -1 2 -3 4 -5 6                    IMP:N,P=1 $indium foil location.
9  100 -2.7  (-10 11 18 -20 21) : (-12 13 -18 19 -20 21 34)
          : (14 -15 -18 19 -20 21 34)
          : (-16 17 -19 -20 21) : (-22 23 20 18)
          : (-24 25 -19 20) : (-26 27 20 -18 19) $ 921
          : (-30 31 -21 18) : (-32 33 -21 -19)
          : (-28 29 -21 -18 19)                IMP:N,P=1 $ Al Shroud
10 100 -2.7 -101 103 -104 (102:-105:106) 107 -108 109 110:
     (102:-105:106) -101 (102:117) -107 111          IMP:n,p=1 $ Aluminum Chamber w/Rest
11 910 -2.65 (-820 821:822 -823) -109               IMP:n,p=1 $ Quartz Window Chamber
15 100 -2.7 -250 251 272 -252                       IMP:n,p=1 $ Elbow
16 100 -2.7 -256 (-222:-255) (102:221) 254 -302 252      IMP:n,p=1 $ Reducer
17 100 -2.624 -270 -272 271                         IMP:n,p=1 $ Turbo Pump
20 200 -0.955 (108 -101 103 -104 (-130:143 -144 (-141:145) (-142:-146)) -212)
     (-133:134:-135 131:136 132:210) #155 #22       IMP:n,p=1 $ Poly Shielding
C 20 200 -0.955 #21 205 -206 207 -208 111 -212 (-201:202:-203:204:213) 150:
C      (108 -101 103 -104 (-130:143 -144 (-141:145) (-142:-146)) -212)
C      (-133:134:-135 131:136 132:210) #155 #22          IMP:n,p=1 $ Poly Shielding
21 600 -1.23E-3  -942 202 -206                      IMP:n,p=1 $ Hole in poly
22 100 -2.7 -130 108 -101 103 -104 (131:132:-133:134) 921 #99  IMP:n,p=1 $ Al Top of Chamber
24 200 -0.955 #21 205 -206 207 -208 111 -212
          (-201:202:-203:204:213) 150               IMP:n,p=1 $ Reflector
C 130 0 (-205:206:-207:208:211) (305 -306 307 -308 209 -311) IMP:n,p=1 $ Lead
30 100 -2.7 -303 302 -111 102:316 -317 -314 315         IMP:n,p=1 $ Aluminum Table
C 41 400 -8.92 411 -421 431 -441 92 -93                 IMP:n,p=1 $ Target Magnets removed -
turned into copper
C 41 300 -7.4 411 -421 431 -441 92 -93                  IMP:n,p=1 $ Target Magnets
C 42 LIKE 41 BUT TRCL=42
C 43 LIKE 41 BUT TRCL=43
C 44 LIKE 41 BUT TRCL=44
51 0 512 -513 514 -515 #1                   u=2    IMP:n,p=1
C  52 0  #51 #61                          u=2    IMP:n,p=1 $ Copper Segment made VOID
52 400 -8.92 #51 #61                       u=2    IMP:n,p=1 $ Copper Segment
```

```
C fill V groove and Water Channel with Copper
61 500 -1.0 -600:-599                    u=2     IMP:n,p=1 $ Water Channel
c 61 500 -1.0  (602:-601) 606:(601:-602) -605      u=2     IMP:n,p=1 $ Water Channel
c 71 400 -8.92 (700 -701:-705 706) 514 -515        u=2     IMP:n,p=1 $ V groove
c 61 500 -1 (602:-601) 606:(601:-602) -605         u=2     IMP:n,p=1 $ Water Channel
c 71 0 (700 -701:-705 706) 514 -515                u=2     IMP:n,p=1 $ V groove
150 0 603 -604 504 -505 u=1 lat=1 fill=-6:6 0:0 0:0
     2 2 2 2 2 2 2 2 2 2 2 2 2 trcl=(-0.25399 0 0)        IMP:n,p=1 $ Target component fill
151 0 90 -91 502 -503 92 -93 fill=1                       IMP:n,p=1 $ Target
152 400 -8.92 ((502 -503 (500 -90:91 -501) 92 -93):
     ((-92 504:93 -505) 500 -501 502 -503))
                #153 #154                 IMP:n,p=1  $ Target Wings      & Caps
153 0 516 -517 514 -515 (500 -90:-501 91)         IMP:n,p=1 $ Wing Slot
154 500 -1 420 -421 440 -441 (-92 94:93 -95)      IMP:n,p=1 $ Target Water Bath
155 100 -2.7 -921 -922 26  505                    IMP:n,p=1
C Cell 100-115 Source Magnets
100 300 -7.4 (120 -122 -124 125 -126 128):        $ Ion Source Magnets
          (-121 123 -124 125 -126 128)        IMP:n,p=1
101 LIKE 100 BUT TRCL=101
102 LIKE 100 BUT TRCL=102
103 LIKE 100 BUT TRCL=103
104 LIKE 100 BUT TRCL=104
105 LIKE 100 BUT TRCL=105
106 LIKE 100 BUT TRCL=106
107 LIKE 100 BUT TRCL=107
108 LIKE 100 BUT TRCL=108
109 LIKE 100 BUT TRCL=109
110 LIKE 100 BUT TRCL=110
111 LIKE 100 BUT TRCL=111
112 LIKE 100 BUT TRCL=112
113 LIKE 100 BUT TRCL=113
114 LIKE 100 BUT TRCL=114
115 LIKE 100 BUT TRCL=115
C Cell 80 Copper Sources
80 400 -8.92 ((800 -802 -110 804):
      (-801 803 -110 804)) #100 #101 #102 #103
      #104 #105 #106 #107 #108 #109
      #110 #111 #112 #113 #114 #115              IMP:n,p=1 $ Ion Source
120 501 1E-6 (800 -802 -804):(-801 803 -804)      IMP:n,p=1 $ Plasma
220   0 -118 (-105 520  : 106 -519 )              IMP:n,p=1 $ Vacuum
221 900 -10.28 ( 519 -800 35 : -520 801 35) -110   IMP:n,p=1 $ Extraction Plate
222 0 ( 519 -800 -35 : -520 801 -35)              IMP:n,p=1 $ Extraction Plate Hole
230 910 -2.65 (802 -812 : -803 813) -110          IMP:n,p=1 $ Quartz Plate
231 100 -2.7  (-105 520 : 106 -519) -110 118      IMP:n,p=1 $ Al Spacer
```

```
C Cell 90 Room Air
90 600 -1.23E-3 (201 -202 203 -204 107 -130 (101:-103:104) (110:812:-813):
    201 -202 203 -204 -107 101 111:
    -150 -212 130 (-143:144:-145 141:146 142):
    150 130 -213 201 -202 203 -204:
    ((-821 201:823 -202) -109):
    209 -909 -907 (932:-931:220) (-934:935) 905 901 -903
    (((-205:206:-207:208:212) 314:317 270:-271):
    -907 -315 209 250 272 (932:-931) 901 -903:
    271 -272 270 -315 209:
    205 -206 207 -208 (-111 (303:-302) (256:222) 255 252:
    315 (-316:314) 250 -252)):907 -908 -910 -940)
    #155                                IMP:n,p=1
91 600 -1.23E-3  -942 907 -946                    IMP:n,p=1  $ Side hole (3")
92 600 -1.23E-3  -945 946 -941                    IMP:n,p=1  $ Side hole (4.5")
93 600 -1.23E-3  -943 941 -908                    IMP:n,p=1  $ Side hole (6")
94 600 -1.23E-3  -944 907 -908                    IMP:n,p=1  $ Angled hole
95 600 -1.23E-3  -940 909 -910                    IMP:n,p=1  $ Top hole
C Concrete Walls
86 800 -2.4 -209 321 912 -914 916 -918 (-902:904:-906:908)  IMP:n,p=1
88 800 -2.4 (909 940:-901:903:-905:907:-209)
      902 -904 906 -908 -910 321
      (943:-941) (942:-907) (945:-946) (944:-907)        IMP:n,p=1
89 800 -2.4 209 -220 931 -907 -932 901                  IMP:n,p=1
87 800 -2.4 220 -909 901 -907 -935 934                  IMP:n,p=1
C Cell 99 - Vacuum Inside
99 0 ((-500:501:-502:503:-504:505) (105 -106:-117) (-221:-254) 252
    -108 (-102:-109 820 -822):-251 -252 272:
    108 133 -134 (135:-131) (-136:-132) -210 -212) #155 #9 IMP:n,p=1
C Beam Stop
1000 201 -0.955     -1000 1010 1020                   IMP:n,p=1
1010 600 -1.23E-3  -1010                            IMP:n,p=1
1020 600 -1.23E-3  -1020                            IMP:n,p=1
C Outside boundary
199 600 -1.23E-3  998 (910:908:904:-902:-906)
              209 -920 -918 -914 912 916 1000         IMP:n,p=1
998 600 -1.23E-3 -998                               IMP:n,p=1
C Non-important Zone outside
999 0 920:918:-916:914:-912:-321                    IMP:n,p=0

C ------------------------------------------------------------------------------
C Surfaces
C ------------------------------------------------------------------------------
C ---------------------------- Shroud Surfaces -------------------------
```

```
C plates with cylindrical caps on top, bottom, and sides, quadrants of spheres cap corners
C ------------------------------------------------------------------------------------
1   PX   2.5
2   PX  -2.5
3   PY   0.01
4   PY  -0.01
5   PZ   2.5
6   PZ   -2.5
10  C/Z  6.7916 0. 3.2385
11  C/Z  6.7916 0. 2.9795
12  PY   3.2385
13  PY   2.9795
14  PY  -3.2385
15  PY  -2.9795
16  C/Z -6.7916 0. 3.2385
17  C/Z -6.7916 0. 2.9795
18  PX   6.7916
19  PX  -6.7916
20  PZ   6.7916
21  PZ  -6.7916
22  S    6.7916 0. 6.7916 3.2385
23  S    6.7916 0. 6.7916 2.9795
24  S   -6.7916 0. 6.7916 3.2385
25  S   -6.7916 0. 6.7916 2.9795
26  C/X  0. 6.7916 3.2385
27  C/X  0. 6.7916 2.9795
28  C/X  0. -6.7916 3.2385
29  C/X  0. -6.7916 2.9795
30  S    6.7916 0. -6.7916 3.2385
31  S    6.7916 0. -6.7916 2.9795
32  S   -6.7916 0. -6.7916 3.2385
33  S   -6.7916 0. -6.7916 2.9795
34  CY   2.032
35  CY   0.15875  $ hole in extraction plate
C  ---------------------------------Vacuum Vessel Surfaces----------------------------
101 CZ  18.503                $ Outer cylindrical surface
102 CZ  15.9                  $ Inner cylindrical surface
103 PY  -9.627                $ Outer planar surface 1
104 PY   9.627                $ Outer planar surface 2  10.281cm
105 PY  -7.087                $ Inner planar surface 1
106 PY   7.087                $ Inner planar surface 2
107 PZ  -14                   $ Bottom Bound
108 PZ   14                   $ Top Bound
109 CX   3.4925               $ Gauge/Equipment Holes
```

```
110 CY   9.5                $ Ion Source Holes
111 PZ  -24                 $ Chamber Rest Bottom Bound
117 PZ  -16                 $ Bottom Chamber Lip bottom
118 CY   4.255               $ Al Spacer
519 PY  10.281               $ Extraction Plate
520 PY -10.281               $ Extraction Plate
130 PZ   16.5               $ HV Insulator
131 C/Z -3.5 0 2
132 C/Z  3.5 0 2
133 PY  -2
134 PY   2
135 PX  -3.5
136 PX   3.5
141 C/Z -3.5 0 4.5
142 C/Z  3.5 0 4.5
143 PY  -4.5
144 PY   4.5
145 PX  -4.5
146 PX   4.5
150 CZ  10
201 PX -20
202 PX 20         $ Shielding Surfaces
203 PY -20
204 PY 20
205 PX -40.32
206 PX 40.32
207 PY -40.32
C For PY and PXs below and above, the oriinal is 40.32 cm. But I extended it to accommodate the
reflector
C It should be brought back at the end of reflector study.
208 PY 40.32
209 PZ -229       $ Floor
210 PZ 44.5
211 PZ 70
212 PZ 47    $original is 47
213 PZ 27
220 PZ -169
221 KZ -64.225 0.2158 1
222 KZ -65 0.2158 1
250 TY -30 0 -46 30 10.3 10.3  $ Elbow
251 TY -30 0 -46 30 10   10
252 PZ -46     $ original -46
253 PZ -42.7
254 CZ 10
```

```
255 CZ 10.3
256 CZ 16.2
270 C/X 0 -76 12.1      $ Turbo Pump
271 PX -59  $original -59
272 PX -30
C Table Surfaces
302 PZ -26.54          $ Bottom of Top Aluminum Frame Shelf
303 CZ 33     $ emeka. 33 is original
314 PZ -55.75
315 PZ -57             $ Bottom of Bottom Al Frame Shelf
316 CZ 28.3          $ original is 28.3
317 CZ 58.2   $ emeka. Original is 58.2 cm
C Lead Outer Surfaces
305 PX -75
306 PX 75
307 PY -75
308 PY 75
311 PZ 75
321 PZ -329     $ Concrete Floor Bottom
325 PX -100
326 PX 100
327 PY -100
328 PY 100
C Concrete Walls
901 PY -233
902 PY -381
903 PY  231
904 PY  479
905 10 PX -232
906 10 PX -288
907 10 PX  232  $original size is 232
908 10 PX  387
909 PZ 197
910 PZ 456
931 10 PX  22
932 PY -74.2 $ original is 60
934 10 PX 125
935 PY -126
940 C/Z 11 -36 7.62       $ Roof Penetration
941 10 PX 335
942 C/X 0 0 3.81       $ 3" to 6" penetration
943 C/X 0 0 7.62
944 900 CX 7.62          $ Angled Penetration
945 C/X 0 0 5.715
```

```
946 10 PX 283
C Outside boundary
912 PY -401
914 PY 499
916 10 PX -308
918 10 PX 707
920 PZ 476
921 CZ 0.95
922 PZ 100
C ------------------------- Beam Stop -------------------------------------
1000 10 RPP 482 562  -30 30  -30 30
1010 10 RCC 482 0 0  25 0 0  10
1020 10 RCC 507 0 0  25 0 0  20
C ------------------------ Target Surfaces --------------------------------
C Target Magnets
411 PX  3.3225
420 PX -3.9575
421 PX  3.9575
431 PY  0.2285
440 PY -0.8440 $-0.8635
441 PY  0.8440 $0.8635
C Target Box
500 PX -4.445
501 PX  4.445
502 PY -0.9525 $-0.8448  $-1.031
503 PY  0.9525 $ 0.8448  $ 1.031
504 PZ -4.66 $-5.08
505 PZ  4.66 $5.08
C Sample Box
512 PY -0.2667 $-0.159
513 PY  0.2667 $0.159
514 PZ -3.175
515 PZ  3.175
516 PY -0.159
517 PY  0.159
C Water Channels
599 C/Z 0. -0.5207 0.1778 $ -0.457 old-y
600 C/Z 0.  0.5207 0.1778 $  0.457
C 601 P 1 0.414 0 0
C 602 P 1 -0.414 0 0
603 PX  -0.254  $-0.357
604 PX   0.254  $ 0.357
605 PY -0.25
606 PY  0.25
```

```
C V-grooves
c 700 P 1 0.414 0 0.09
c 701 P 1 -0.414 0 -0.09
C 700 PX  0.357
C 701 PX -0.357
C 702 PZ -3.105
C  703 PZ 3.105
c 705 P 1 0.414 0 -0.09
c 706 P 1 -0.414 0 0.09
C   705 PX -0.357
C   706 PX  0.357
90 PX  -2.54 $-2.286 $ -3.213 $ Non-universe target surfaces
91 PX   2.54 $ 3.213
92 PZ -3.81
93 PZ  3.81
94 PZ -4.29
95 PZ  4.29
C Ion Sources Surfaces
800 PY  10.598 $9.9445 $9.3095  $7.4
801 PY -10.598 $-9.9445 $-9.3095 $-7.4
802 PY 16.313 $15.8575  $15.54   $13.3
803 PY -16.313 $-15.8575 $-15.54  $-13.3
804 CY 6.19
812 PY 16.948  $ 16.64 $14.1
813 PY -16.948 $-16.64 $-14.1
C Ion Source Magnet
120 PY  10.8907 $10.575  $8.035      $ Ion Source Magnets
121 PY -10.9907 $-10.575 $-8.035
122 PY  14.7025  $14.385  $11.845
123 PY -14.7025 $-14.385 $-11.845
124 PX 0.635
125 PX -0.635
126 PZ 8.447
127 PZ -8.447
128 PZ 7.177
129 PZ -7.177
C ----------------------
820 PX -17.36          $ Quartz Window Chamber
821 PX -18
822 PX 17.36
823 PX 18
C ----------------------
998 RCC 227.0001 0 0 .0001 0 0 3.81
C Reflector
```

```
11901 PX 20
11902 PX -20
11903 PY 37
11904 PY 22
11905 PZ -13
11906 PZ 13

C -------------------------------------------------------------------------
C Data
C -------------------------------------------------------------------------
TR10 -170 0 0   $ Room transformation to accomodate generator
C Magnet Coordinate Transformations
TR4   0     -0.05    0
TR42  -7.28   0      0
TR43  0      -1.092  0
TR44  -7.28  -1.092  0
TR62  -0.714  0      0
TR63  -1.428  0      0
TR64  -2.142  0      0
TR65   0.714  0      0
TR66   1.428  0      0
TR67   2.142  0      0
TR68   2.856  0      0
TR72  -0.714  0      0
TR73  -1.428 0 0
TR74  -2.142 0 0
TR75  -2.856 0 0
TR76   0.714 0 0
TR77   1.428 0 0
TR78   2.142 0 0
TR79   2.856 0 0
TR101  0 0 0 0.9239 0 -0.3827 0 1 0 0.3827 0 0.9239
TR102  0 0 0 0.7071 0 -0.7071 0 1 0 0.7071 0 0.7071
TR103  0 0 0 0.3827 0 -0.9239 0 1 0 0.9239 0 0.3827
TR104  0 0 0 0 0 -1 0 1 0 1 0 1
TR105  0 0 0 -0.3827 0 -0.9239 0 1 0 0.9239 0 -0.3827
TR106  0 0 0 -0.7071 0 -0.7071 0 1 0 0.7071 0 -0.7071
TR107  0 0 0 -0.9239 0 -0.3827 0 1 0 0.3827 0 -0.9239
TR108  0 0 0 -1 0 0 0 1 0 0 0 -1
TR109  0 0 0 -0.9239 0 0.3827 0 1 0 -0.3827 0 -0.9239
TR110  0 0 0 -0.7071 0 0.7071 0 1 0 -0.7071 0 -0.7071
TR111  0 0 0 -0.3827 0 0.9239 0 1 0 -0.9239 0 -0.3827
TR112  0 0 0 0 0 1 0 1 0 -1 0 0
TR113  0 0 0 0.3827 0 0.9239 0 1 0 -0.9239 0 0.3827
```

```
TR114  0 0 0 0.7071 0 0.7071 0 1 0 -0.7071 0 0.7071
TR115  0 0 0 0.9239 0 0.3827 0 1 0 -0.3827 0 0.9239
TR900  62 -41 51 0.707 0.707 0 -0.707 0.707 0 0 0 1
C ------------------------------------------------------------------------------
C Materials for Geometry-----------------------------------------------------
C ------------------------------------------------------------------------------
M50 49113 0.0429 49115 0.9571     $ Natural Indium
M60 49115   1.0     $ In-115
M100   13027 1 $ Aluminum
M200   6000  0.3333 $ Polyethylene
      1001  0.6667
M201   6000  37.5  $ Polyethylene + Boron 5 percent weight
      1001  74.985
      1002  0.015
      5010  0.588 $ B-10
      5011  2.412 $ B-11
M300   60142 0.032 $ Nd-Fe-B Magnets
      60143 0.014
      60144 0.028
      60145 0.010
      60146 0.020
      60148 0.007
      60150 0.007
      26054 0.047792
      26056 0.755773
      26057 0.018128
      26058 0.002307
      5010  0.0116
      5011  0.0464
M301 26054 1
M302 26058 1
M303 60142 1
M304 60143 1
M305 60144 1
M306 60146 1
M400  29063 0.6915 $ Copper-63
     29065 0.3085 $ Copper-65
M401  29063 1
M402  29065 1
M500  1001 0.667 $ Water
     8016 0.333
M501  1002 1
M600  8016       -0.232       $ Dry Air
     7014       -0.754
```

```
     18040      -0.014
C M700  82000 1 $ Lead
M800  1001  -0.0221   $ Concrete
     6000  -0.002484
     8016  -0.574930
     11023 -0.015208
     12024 -0.001000013
     12025 -0.0001266
     12026 -0.000139387
     13027 -0.019953
     14028  -0.280936158
     14029  -0.014271775
     14030  -0.009419067
     19039 -0.009367776
     19041 -0.000677224
          20040 -0.041719165
          20042 -0.000277893
     20043 -0.000057984
     20044         -0.000895958
     26054   -0.000376126
     26056   -0.00590437
     26057   -0.000136358
     26058          -0.000018147
M900  42092  0.1484    $ Moly plate
     42094  0.0925
     42095  0.1592
     42096  0.1668
     42097  0.0955
     42098  0.2413
     42100  0.0963
M901  42098  1
M910  14028 0.3074      $ Quartz
     14029 0.0156
     14030 0.0103
     8016 0.6667
M911  14030 1
C **********REFLECTOR MATERIALS**********
 M9112 6012 1. $Carbon
 M9113 20040 1. $Ca-40
 M9114 82208 1. $Pb-208
 M9115 20040 0.1939   $ Calcium Carbonate.
     20040 0.001294
     20040 0.00027
     20040 0.004172
```

```
     6012  0.1979
     6013  0.00214
     8016  0.5985
     8016  0.00023
     8016  0.00123
M9116 26056 1. $Iron
M9117 6000 1. $natural Carbon
M9118 26054   0.05845  $natural Iron
     26056   0.91754
     26057   0.02119
     26058          0.00282
M9119 82204   0.014  $natural Pb
           82206   0.241
     82207   0.221
     82208   0.524
M9120 5010 1. $Boron
C Scattering Kernels
C MT100 al27 $ Aluminum
C MT200 poly $ natural polyethylene
C MT201 poly $ borated polyethylene
C MT300 fe56 $ Iron
C MT500 lwtr $ Hydrogen in Light Water
C ------------------------------------------------------------------------------
C ---- Mesh Tallies ----- When using 2 sources the factor below should be doubled
C ------------------------------------------------------------------------------
C FMESH14:N origin=0 -401 -2.5 imesh=540 jmesh=499 kmesh=2.5
C         iints=108 jints=180 kints=1 factor=1.08e08
C DE14   1.0E-9 1.0E-8 2.5E-8 1.0E-7 2.0E-7 5.0E-7 1.0E-6 2.0E-6 5.0E-6
C      1.0E-5 2.0E-5 5.0E-5 1.0E-4 2.0E-4 5.0E-4 1.0E-3 2.0E-3 5.0E-3
C      0.0100 0.0200 0.0300 0.0500 0.0700 0.1000 0.1500 0.2000 0.3000
C      0.5000 0.7000 0.9000 1.0000 1.2000 1.5000 2.0000 3.0000
C DF14   1.7    2.03   2.31   2.98   3.36   3.86   4.17   4.40   4.59
C      4.68   4.72   4.73   4.72   4.67   4.60   4.58   4.61   4.86
C      5.57   7.41   9.46   13.7   18.0   24.3   34.7   44.7   63.8
C      99.1   131    160    174    193    219    254    301
C FMESH24:P origin=0 -401 -2.5 imesh=540 jmesh=499 kmesh=2.5
C         iints=108 jints=180 kints=1 factor=1.08e08
C DE24   0.010 0.015 0.020 0.030 0.040 0.050 0.060 0.070 0.080 0.100 0.150
C      0.200 0.300 0.400 0.500 0.511 0.600 0.662 0.800 1.000 1.117 1.333
C      1.500 2.000 3.000 4.000 5.000 6.000 6.129 8.000 10.00 15.00 20.00
C DF24   .0337 .0664 .0986 0.158 0.199 0.226 0.248 0.273 0.297 0.355 0.528
C      0.721 1.120 1.520 1.920 1.960 2.300 2.540 3.040 3.720 4.100 4.750
C      5.240 6.550 8.840 10.80 12.70 14.40 14.60 17.60 20.60 27.70 34.40
C FMESH34:N origin=-40 -40 -40 imesh=40 jmesh=40 kmesh=40
```

```
C       iints=40 jints=40 kints=40 factor=1.0e08
C DE34   0.010 0.015 0.020 0.030 0.040 0.050 0.060 0.070 0.080 0.100 0.150
C       0.200 0.300 0.400 0.500 0.511 0.600 0.662 0.800 1.000 1.117 1.333
C       1.500 2.000 3.000 4.000 5.000 6.000 6.129 8.000 10.00 15.00 20.00
C DF34   .0337 .0664 .0986 0.158 0.199 0.226 0.248 0.273 0.297 0.355 0.528
C       0.721 1.120 1.520 1.920 1.960 2.300 2.540 3.040 3.720 4.100 4.750
C       5.240 6.550 8.840 10.80 12.70 14.40 14.60 17.60 20.60 27.70 34.40
C FMESH44:N origin=-40 -40 -40 imesh=40 jmesh=40 kmesh=40
C       iints=40 jints=40 kints=40 factor=1.0e08
C FMESH64:N geom=cyl origin = 217. 0. 0. axs=0 1 0 vec=0 0 1
C               imesh=7.62 jmesh=0.25 kmesh=1
C               iints=1 jints=1 kints=1
C FMESH74:N geom=cyl origin = 0.0 1.62 0.0 axs=0 1 0 vec=0 0 1
C               imesh=1 jmesh=0.0001 kmesh=1
C               iints=1 jints=1 kints=1 emesh=3. eints=200
C FMESH104:N geom=cyl origin= 0. -0.065 0. axs=0 1 0 vec=1 0 0
C               imesh=0.425 jmesh=0.025 kmesh=1
C               iints=1 jints=1 kints=1 emesh=3. eints=1200
C FMESH114:N geom=cyl origin= 1.0 -0.065 0. axs=0 1 0 vec=1 0 0
C               imesh=0.425 jmesh=0.025 kmesh=1
C               iints=1 jints=1 kints=1 emesh=3. eints=1200
C FMESH144:N geom=cyl origin= 1. -0.065 1. axs=0 1 0 vec=1 0 0
C              imesh=0.425 jmesh=0.025 kmesh=1
C               iints=1 jints=1 kints=1 emesh=3. eints=1200
C FMESH154:N geom=cyl origin= 0. 16.95 0. axs=0 1 0 vec=1 0 0
C               imesh=1.0 jmesh=0.025 kmesh=1
C               iints=1 jints=1 kints=1 emesh=3. eints=1200
C     #####
E0 0 200i 3
F11:n (1 2 3 4 5 6)
C11 0 1
C F21:n 4
C F14:n 1
C FMESH14:N geom=cyl origin = 0 0 0 axs = 0 1 0 vec = 1 0 0
C               imesh=0.495 jmesh=0.05 kmesh=1
C               iints=1 jints=1 kints=1 emesh=0.4 1 &
C                                       1.1 1.3 1.6 1.8 2 2.9 &
C                                       eints= 1 12 1 1 1 1 1 9
C               factor 0.03848 $ volume of the fmesh
C FM14 0.03827
C
FMESH64:N geom=cyl origin = 0.189 0 0.11 axs = 0 1 0 vec = 1 0 0
               imesh=0.495 jmesh=0.05 kmesh=1
               iints=1 jints=1 kints=1 emesh=0.4 2.8
```

```
                                        eints= 1 240
                factor 0.03848 $ volume of the fmesh
FM64 0.03827  $ multiply with atom density in per barn-cm
FMESH4:N geom=cyl origin = 0.189 0 0.11 axs = 0 1 0 vec = 1 0 0
                imesh=0.495 jmesh=0.05 kmesh=1
                iints=1 jints=1 kints=1 emesh=3. eints=200
                factor 0.03848 $ volume of the fmesh
FM4 0.03827 50 102
C
C Source - 0.25 cm radius disk sources located
C          outside the copper target holder
C
C SDEF POS=-0.05 -0.37 -0.686  &
C SDEF POS=0. 0. -0.686  &
C     AXS=0 0 1 VEC=0 0 1 RAD=D3 PAR=N DIR=D4 ERG=fdir D5 &
C     WGT=1.0 EXT=0
SDEF POS = 0.0 -1 0.0 &
    AXS=0 0 1 VEC=0 1 0 RAD=D3 PAR=1 DIR=D4 ERG=fdir D5 &
    WGT=1.0  EXT=0
C SI1 L  0 -1.1 0.  0 1.1 0.
C SP1 0.5  0.5
C  Distribution for axs
C SIn L 0 1 0 0 -1 0
C SPn 0.5 0.5
C  Distribution for vec
C  DS2 L 0 0 1
C  Distribution for rad
SI3   0 0.25
SP3 -21 1.0
C   Distribution for dir
C   This is cos(theta) in one-degree increments from 180 to 0 degreesou
C
SI4   -1    -0.99985    -0.99939    -0.99863    -0.99756 &
-0.99619    -0.99452    -0.99255    -0.99027    -0.98769 &
-0.98481    -0.98163    -0.97815    -0.97437     -0.9703 &
-0.96593    -0.96126     -0.9563    -0.95106    -0.94552 &
-0.93969    -0.93358    -0.92718     -0.9205    -0.91355 &
-0.90631    -0.89879    -0.89101    -0.88295    -0.87462 &
-0.86603    -0.85717    -0.84805    -0.83867    -0.82904 &
-0.81915    -0.80902    -0.79864    -0.78801    -0.77715 &
-0.76604    -0.75471    -0.74314    -0.73135    -0.71934 &
-0.70711    -0.69466     -0.682    -0.66913    -0.65606 &
-0.64279    -0.62932    -0.61566    -0.60182    -0.58779 &
-0.57358    -0.55919    -0.54464    -0.52992    -0.51504 &
```

```
-0.5       -0.48481    -0.46947    -0.45399    -0.43837 &
-0.42262    -0.40674    -0.39073    -0.37461    -0.35837 &
-0.34202    -0.32557    -0.30902    -0.29237    -0.27564 &
-0.25882    -0.24192    -0.22495    -0.20791    -0.19081 &
-0.17365    -0.15643    -0.13917    -0.12187    -0.10453 &
-0.087156   -0.069756   -0.052336   -0.034899   -0.017452 &
6.1232e-17   0.017452    0.034899    0.052336    0.069756 &
0.087156     0.10453     0.12187     0.13917     0.15643 &
0.17365     0.19081     0.20791     0.22495     0.24192 &
0.25882     0.27564     0.29237     0.30902     0.32557 &
0.34202     0.35837     0.37461     0.39073     0.40674 &
0.42262     0.43837     0.45399     0.46947     0.48481 &
0.5        0.51504     0.52992     0.54464     0.55919 &
0.57358     0.58779     0.60182     0.61566     0.62932 &
0.64279     0.65606     0.66913      0.682     0.69466 &
0.70711     0.71934     0.73135     0.74314     0.75471 &
0.76604     0.77715     0.78801     0.79864     0.80902 &
0.81915     0.82904     0.83867     0.84805     0.85717 &
0.86603     0.87462     0.88295     0.89101     0.89879 &
0.90631     0.91355      0.9205     0.92718     0.93358 &
0.93969     0.94552     0.95106      0.9563     0.96126 &
0.96593      0.9703     0.97437     0.97815     0.98163 &
0.98481     0.98769     0.99027     0.99255     0.99452 &
0.99619     0.99756     0.99863     0.99939     0.99985 &
1.0
C
C   ------------------------------------------------------------------------------
C   This is the secondary neutron angular distribution for incident deuterons of initial
C   energy of 100keV - uses Cory's reaction # to weight slowing down spectrum
C   (dsigma/domega)(theta)*domega normalized
C     From Liskiien -Paulsen
C   Error in previous computation - now corrected here
C   ------------------------------------------------------------------------------
SP4 0.000000000  0.000094925  0.000284665  0.000474124  0.000663135  &
0.000851536  0.001039164  0.001225856  0.001411450  0.001595787  &
0.001778707  0.001960052  0.002139668  0.002317400  0.002493096  &
0.002666609  0.002837791  0.003006499  0.003172594  0.003335940  &
0.003496403  0.003653857  0.003808177  0.003959246  0.004106950  &
0.004251182  0.004391841  0.004528831  0.004662064  0.004791458  &
0.004916940  0.005038441  0.005155905  0.005269279  0.005378522  &
0.005483600  0.005584487  0.005681169  0.005773637  0.005861895  &
0.005945953  0.006025832  0.006101562  0.006173183  0.006240742  &
0.006304297  0.006363913  0.006419665  0.006471636  0.006519917  &
0.006564607  0.006605812  0.006643644  0.006678224  0.006709676  &
```

```
0.006738133 0.006763730 0.006786608 0.006806913 0.006824792 &
0.006840396 0.006853879 0.006865397 0.006875103 0.006883157 &
0.006889712 0.006894925 0.006898950 0.006901939 0.006904042 &
0.006905404 0.006906170 0.006906477 0.006906460 0.006906249 &
0.006905968 0.006905734 0.006905659 0.006905850 0.006906404 &
0.006907414 0.006908964 0.006911131 0.006913985 0.006917587 &
0.006921990 0.006927242 0.006933379 0.006940432 0.006948423 &
0.006957366 0.006967266 0.006978123 0.006989926 0.007002659 &
0.007016296 0.007030806 0.007046149 0.007062279 0.007079141 &
0.007096675 0.007114813 0.007133483 0.007152602 0.007172086 &
0.007191841 0.007211768 0.007231762 0.007251715 0.007271510 &
0.007291025 0.007310136 0.007328710 0.007346613 0.007363703 &
0.007379835 0.007394861 0.007408626 0.007420975 0.007431745 &
0.007440774 0.007447895 0.007452937 0.007455728 0.007456095 &
0.007453861 0.007448849 0.007440880 0.007429777 0.007415359 &
0.007397449 0.007375870 0.007350445 0.007321001 0.007287368 &
0.007249376 0.007206863 0.007159670 0.007107642 0.007050632 &
0.006988499 0.006921108 0.006848335 0.006770061 0.006686181 &
0.006596595 0.006501218 0.006399974 0.006292801 0.006179649 &
0.006060480 0.005935271 0.005804014 0.005666714 0.005523393 &
0.005374087 0.005218848 0.005057745 0.004890862 0.004718300 &
0.004540175 0.004356622 0.004167788 0.003973840 0.003774957 &
0.003571336 0.003363187 0.003150736 0.002934220 0.002713892 &
0.002490016 0.002262869 0.002032735 0.001799913 0.001564708 &
0.001327433 0.001088409 0.000847961 0.000606422 0.000364126 &
0.000121410
C    ------------------------------------------
C     Neutron energy vs angle wtd as above
C    ------------------------------------------
DS5 2.1751  2.1752  2.1753  2.1755  2.1758  &
2.1762  2.1767  2.1773  2.1779  2.1787  &
2.1795  2.1804  2.1814  2.1825  2.1837  &
2.1849  2.1863  2.1877  2.1892  2.1908  &
2.1925  2.1942  2.1961  2.1980  2.2000  &
2.2021  2.2042  2.2065  2.2088  2.2112  &
2.2137  2.2162  2.2188  2.2215  2.2243  &
2.2271  2.2301  2.2330  2.2361  2.2392  &
2.2424  2.2457  2.2490  2.2524  2.2559  &
2.2594  2.2630  2.2666  2.2703  2.2741  &
2.2779  2.2818  2.2858  2.2898  2.2938  &
2.2979  2.3021  2.3063  2.3106  2.3149  &
2.3192  2.3237  2.3281  2.3326  2.3372  &
2.3418  2.3464  2.3511  2.3558  2.3605  &
2.3653  2.3702  2.3750  2.3799  2.3849  &
```

```
2.3898  2.3948  2.3999  2.4049  2.4100  &
2.4151  2.4202  2.4254  2.4306  2.4358  &
2.4410  2.4462  2.4515  2.4568  2.4621  &
2.4674  2.4727  2.4780  2.4833  2.4887  &
2.4940  2.4994  2.5047  2.5101  2.5154  &
2.5208  2.5261  2.5315  2.5368  2.5421  &
2.5475  2.5528  2.5581  2.5634  2.5686  &
2.5739  2.5791  2.5843  2.5895  2.5947  &
2.5998  2.6050  2.6101  2.6151  2.6201  &
2.6251  2.6301  2.6350  2.6399  2.6447  &
2.6495  2.6542  2.6589  2.6636  2.6682  &
2.6727  2.6772  2.6817  2.6860  2.6904  &
2.6946  2.6988  2.7030  2.7070  2.7110  &
2.7149  2.7188  2.7226  2.7263  2.7299  &
2.7335  2.7369  2.7403  2.7436  2.7469  &
2.7500  2.7530  2.7560  2.7589  2.7616  &
2.7643  2.7669  2.7694  2.7718  2.7741  &
2.7763  2.7784  2.7804  2.7823  2.7841  &
2.7858  2.7874  2.7888  2.7902  2.7915  &
2.7926  2.7937  2.7946  2.7955  2.7962  &
2.7968  2.7973  2.7977  2.7980  2.7981  &
2.7982
C  SP3    0. 0.01  0.99
C  SI3 -1 .992532 1   $ 7-degree cone towards hole, biased by 20x
C  SP3 0 0.996266 .003734
C  SB3 0 .05 .95
C FMESH tallys
FMESH2224:N geom=cyl origin = 0.189 0 1.11 axs = 0 1 0 vec = 1 0 0
            imesh=0.495 jmesh=0.05 kmesh=1
            iints=1 jints=1 kints=1 emesh=0.4 2.8
                                    eints= 1 240
                                    factor 0.03848 $ volume of the fmesh
FM2224 0.03827
FMESH2234:N geom=cyl origin = 0.189 0 1.11 axs = 0 1 0 vec = 1 0 0
            imesh=0.495 jmesh=0.05 kmesh=1
            iints=1 jints=1 kints=1 emesh=3. eints=200
                                    factor=0.03848 $ volume of the fmesh
 FM2234 0.03827 50 102
FMESH2244:N geom=cyl origin = 1.189 0 0.11 axs = 0 1 0 vec = 1 0 0
            imesh=0.495 jmesh=0.05 kmesh=1
            iints=1 jints=1 kints=1 emesh=0.4 2.8
                                    eints= 1 240
                                    factor 0.03848 $ volume of the fmesh
FM2244 0.03827
```

```
FMESH2254:N geom=cyl origin = 1.189 0 0.11 axs = 0 1 0 vec = 1 0 0
          imesh=0.495 jmesh=0.05 kmesh=1
          iints=1 jints=1 kints=1 emesh=3. eints=200
                                  factor=0.03848 $ volume of the fmesh
 FM2254 0.03827 50 102
FMESH2264:N geom=cyl origin = 1.189 0 1.11 axs = 0 1 0 vec = 1 0 0
          imesh=0.495 jmesh=0.05 kmesh=1
          iints=1 jints=1 kints=1 emesh=0.4 2.8
                                  eints= 1 240
                                  factor 0.03848 $ volume of the fmesh
FM2264 0.03827
FMESH2274:N geom=cyl origin = 1.189 0 1.11 axs = 0 1 0 vec = 1 0 0
          imesh=0.495 jmesh=0.05 kmesh=1
          iints=1 jints=1 kints=1 emesh=3. eints=200
                                  factor=0.03848 $ volume of the fmesh
 FM2274 0.03827 50 102
FMESH2284:N geom=cyl origin = -0.811 0 0.11 axs = 0 1 0 vec = 1 0 0
          imesh=0.495 jmesh=0.05 kmesh=1
          iints=1 jints=1 kints=1 emesh=0.4 2.8
                                  eints= 1 240
                                  factor 0.03848 $ volume of the fmesh
FM2284 0.03827
FMESH2294:N geom=cyl origin = -0.811 0 0.11 axs = 0 1 0 vec = 1 0 0
          imesh=0.495 jmesh=0.05 kmesh=1
          iints=1 jints=1 kints=1 emesh=3. eints=200
                                  factor=0.03848 $ volume of the fmesh
 FM2294 0.03827 50 102
FMESH3324:N geom=cyl origin = 0.189 0 -0.89 axs = 0 1 0 vec = 1 0 0
          imesh=0.495 jmesh=0.05 kmesh=1
          iints=1 jints=1 kints=1 emesh=0.4 2.8
                                  eints= 1 240
                                  factor 0.03848 $ volume of the fmesh
FM3324 0.03827
FMESH3334:N geom=cyl origin = 0.189 0 -0.89 axs = 0 1 0 vec = 1 0 0
          imesh=0.495 jmesh=0.05 kmesh=1
          iints=1 jints=1 kints=1 emesh=3. eints=200
                                  factor=0.03848 $ volume of the fmesh
 FM3334 0.03827 50 102
FMESH3354:N geom=cyl origin = -0.811 0 -0.89 axs = 0 1 0 vec = 1 0 0
          imesh=0.495 jmesh=0.05 kmesh=1
          iints=1 jints=1 kints=1 emesh=0.4 2.8
                                  eints= 1 240
                                  factor 0.03848 $ volume of the fmesh
FM3354 0.03827
```

```
FMESH3364:N geom=cyl origin = -0.811 0 -0.89 axs = 0 1 0 vec = 1 0 0
          imesh=0.495 jmesh=0.05 kmesh=1
          iints=1 jints=1 kints=1 emesh=3. eints=200
                                  factor=0.03848 $ volume of the fmesh
 FM3364 0.03827 50 102
FMESH3374:N geom=cyl origin = -0.811 0 1.11 axs = 0 1 0 vec = 1 0 0
          imesh=0.495 jmesh=0.05 kmesh=1
          iints=1 jints=1 kints=1 emesh=0.4 2.8
                                  eints= 1 240
                                  factor 0.03848 $ volume of the fmesh
FM3374 0.03827
FMESH3384:N geom=cyl origin = -0.811 0 1.11 axs = 0 1 0 vec = 1 0 0
          imesh=0.495 jmesh=0.05 kmesh=1
          iints=1 jints=1 kints=1 emesh=3. eints=200
                                  factor=0.03848 $ volume of the fmesh
 FM3384 0.03827 50 102
FMESH3394:N geom=cyl origin = 1.189 0 -0.89 axs = 0 1 0 vec = 1 0 0
          imesh=0.495 jmesh=0.05 kmesh=1
          iints=1 jints=1 kints=1 emesh=0.4 2.8
                                  eints= 1 240
                                  factor 0.03848 $ volume of the fmesh
FM3394 0.03827
FMESH4404:N geom=cyl origin = 1.189 0 -0.89 axs = 0 1 0 vec = 1 0 0
          imesh=0.495 jmesh=0.05 kmesh=1
          iints=1 jints=1 kints=1 emesh=3. eints=200
                                  factor=0.03848 $ volume of the fmesh
FM4404 0.03827 50 102
C FCL:n 1 1 0 34i 0
RAND GEN=2 STRIDE=152917 SEED=10899028731
NPS  1e9
C CUT:n j 1.5e-8
MODE n
C PTRAC  file=asc write=all event=src
VOID 24
PRINT 110
C PRDMP 2J 1
```

Appendix B
MCNP output processing scripts

Python scripts that processes the output of the mcnp simulation. The script loads the MCNP meshatal output file and gets the reaction rate or neutron flux.

```
#For absence of polyethylene plates
import numpy as np
import os
from math import log10, floor

def is_number(n):
    try:
        float(n)   # Type-casting the string to `float`.
                   # If string is not a valid `float`,
                   # it'll raise `ValueError` exception
    except ValueError:
        return False
    return True

def round_to_n(x,n):
    return round(x, -int(floor(log10(abs(x))))+(n-1))

count = 1
foil = []
flux1 = []
n_atoms = []
In115m = []
In115m_error = []
In116m = []
In116m_error = []
# Loads the cross-section
CS = np.loadtxt("In115 CS")
#extracts data from MCNP output
#first enter file name here.
file_name = "negative x positive y/1Billion_endf_vii_meshtalFullHFNGNORef_endf_vii_latest.txt"
with open(file_name) as file:
    for line in file:
        if line.strip():
            count+=1
            val = line.split()
            if is_number(val[0]):
```

```
            foil.append(float(val[4])) #gets the flux or number of particles produced
            if float(val[0])==2.8: # trigers the sellection of fluxes (for In-115m).
               temp = foil.copy()
               In115_atoms = np.multiply(temp,CS)
               In115m.append(In115_atoms.sum()) #sums the In-115m atoms
               total = next(file)
               In115m_error.append(total.split()[5]) #grabs and append the error
               foil[:] = [] # empties the list
            if float(val[0])==3.0:# trigers the sellection of number of atoms (In-116m)
               temp = foil.copy()
               In116_atoms = np.multiply(temp,1) #multiplies number of In116m atom by B.R.
               In116m.append(In116_atoms.sum()) #sums the In-116m atoms
               total = next(file) # goest to the next line in the open file
               In116m_error.append(float(total.split()[5])) #grabs and appends the error
               foil[:] = []
In116m_no_poly = np.multiply(In116,0.79)
sortedIndex = [7,1,3,4,0,2,6,5,8]
In116m_right_order_no_poly = [In116m_no_poly[i] for i in sortedIndex]
In116m_right_order_no_poly_error = [In116_error[i] for i in sortedIndex]
In115m_right_order_no_poly = [In115m[i] for i in sortedIndex]
In115m_right_order_no_poly_error = [In116m_error[i] for i in sortedIndex]
print("Foil\tIn116m reaction rate","\tFrac. error","\tIn115m reaction rate","\tFrac. error")
for i in range(9):
   print(i+1,"\t",round_to_n(In116m_right_order_no_poly[i],3),"\t\t",\
        round_to_n(In116m_right_order_no_poly_error[i],3),\
       "\t",round_to_n(In115m_right_order_no_poly[i],3),"\t\t",\
        round_to_n(In115m_right_order_no_poly_error[i],3))
```

```
#For presence of polyethylene plates
import numpy as np
import os
from math import log10, floor

def is_number(n):
    try:
        float(n)   # Type-casting the string to `float`.
                   # If string is not a valid `float`,
                   # it'll raise `ValueError` exception
    except ValueError:
        return False
    return True

def round_to_n(x,n):
    return round(x, -int(floor(log10(abs(x))))+(n-1))

count = 1
foil = []
flux1 = []
n_atoms = []
In115m = []
In115m_error = []
In116m = []
In116m_error = []
# Loads the cross-section
CS = np.loadtxt("In115 CS")
#extracts data from MCNP output
#first enter file name here.
file_name = "negative x positive y/1Billion_endf_vii_meshtalFullHFNGPoly_endf_vii_latest.txt"
with open(file_name) as file:
    for line in file:
        if line.strip():
            count+=1
            val = line.split()
            if is_number(val[0]):
                foil.append(float(val[4])) #gets the flux or number of particles produced
                if float(val[0])==2.8: # trigers the sellection of fluxes (for In-115m).
                    temp = foil.copy()
                    In115_atoms = np.multiply(temp,CS)
                    In115m.append(In115_atoms.sum()) #sums the In-115m atoms
                    total = next(file)
                    In115m_error.append(total.split()[5]) #grabs and append the error
                    foil[:] = [] # empties the list
```

```
            if float(val[0])==3.0:# trigers the sellection of number of atoms (In-116m)
                temp = foil.copy()
                In116_atoms = np.multiply(temp,1) #multiplies number of In116m atoms by B.R.
                In116m.append(In116_atoms.sum()) #sums the In-116m atoms
                total = next(file) # goest to the next line in the open file
                In116m_error.append(float(total.split()[5])) #grabs and appends the error
                foil[:] = []
In116m_poly = np.multiply(In116m,0.79)
sortedIndex = [7,1,3,4,0,2,6,5,8]
In116m_right_order_poly = [In116m_poly[i] for i in sortedIndex]
In116m_right_order_poly_error = [In116_error[i] for i in sortedIndex]
In115m_right_order_poly = [In115m[i] for i in sortedIndex]
In115m_right_order_poly_error = [In116m_error[i] for i in sortedIndex]
print("Foil\tIn116m reaction rate","\tFrac. error","\tIn115m reaction rate","\tFrac. error")
for i in range(9):
   print(i+1,"\t",round_to_n(In116m_right_order_poly[i],3),"\t\t",\
        round_to_n(In116m_right_order_poly_error[i],3),\
       "\t",round_to_n(In115m_right_order_poly[i],3),"\t\t",\
        round_to_n(In115m_right_order_poly_error[i],3))
```